Study of Thermal Stratification for Pressurizer Surge Line of Pressurizer Water Reactor

By

Abdullah

NUST201463524MCES64114F

Session 2014-16

Supervised by

Dr. Majid Ali

A thesis submitted to the US Pakistan Center for Advance Studies in Energy in partial fulfillment of the requirements for the degree of

Master of Science

In

ENERGY SYSTEM ENGINEERING

US Pakistan Center for Advance Studies in Energy (USPCAS-E)

National University of Science and Technology (NUST)

H-12, Islamabad 44000, Pakistan

August 2018

THESIS ACCEPTANCE CERTIFICATE

Certified that final copy of MS thesis written by Mr. Abdullah, (Registration No. NUST201463524MCES64114F), of US Pakistan Center for Advance Studies in Energy has been vetted by undersigned, found complete in all respects as per NUST Statues/Regulations, is free of plagiarism, errors, and mistakes and is accepted as partial fulfillment for award of MS degree. It is further certified that necessary amendments as pointed out by GEC members of the scholar have also been incorporated in the said thesis.

Signature: _____

Name of Supervisor: Dr. Majid Ali

Date: _____

Signature (HoD): _____

Date: _____

Signature (Dean/Principal): _____

Date: _____

Certificate

This is to certify that work in this thesis has been carried out by **Mr. Abdullah** and completed under my supervision in US Pakistan Centre for Advance Studies in Energy (USPCAS-E), National University of Sciences and Technology, H-12, Islamabad, Pakistan.

Supervisor:	Dr. Majid Ali US Pakistan Centre for Advance Studies in Energy, NUST, Islamabad
GEC Member # 1:	Dr. Adeel Waqas US Pakistan Centre for Advance Studies in Energy NUST, Islamabad
GEC Member # 2	Dr. Naseem Iqbal US Pakistan Centre for Advance Studies in Energy NUST, Islamabad
HoD-ESE	Dr. Naseem Iqbal US Pakistan Centre for Advance Studies in Energy NUST, Islamabad
Principal/ Dean	Dr. Zuhair S. Khan US Pakistan Centre for Advance Studies in Energy, NUST, Islamabad

Dedicated to

To my loving parents whom prayers are always ahead of me.

To my compassionate supervisor and teacher Dr. Majid Ali. Whose constant guidance and regular Motivation's has led me to complete My MS degree.

List of Figures

Figure 1World Electricity Consumption[6] III
Figure 2 Layout of typical PWR [9]..... 1
Figure 3 label diagram of typical PWR..... 2
Figure 4 Typical layout of pressurizer surge..... 2
Figure 5 Surge line layout 1 [10] 3
Figure 6 Surge line layout 2 [11] 3
Figure 7 Surge line layout 4[13]-[14] 4
Figure 8 Surge line layout 3 [12] 4
Figure 9 Surge line layout 8 [15] 4
Figure 10 Transient Temperature Profile of Diablo Canyon Surge Line [9] 15
Figure 11 Transient Temperature Profile of San Onfore Surge Line [10] 16
Figure 12 Top to bottom temperature difference during heat up [10] 17
Figure 13 Deformation of complete solid element model [1]..... 22
Figure 14 Pressurizer Surge Line Model (Left) and Deformation (Right) [5]..... 23
Figure 15 Temperature Distribution in Pressurizer Surge Line Cross Section [1] 23
Figure 16 Finite Element Model and Comparison of Circumferential Temperature [3] 24
Figure 17 Comparison of Temperature Difference Change between No Heating and External [15]..... 25
Figure 18 Pressurizer surge line model of VVER-440 and meshed T-Junction [17] 26
Figure 19 Measured and calculated coolant temperatures in the pressurizer surge line at monitor line 0 and 4 [17]..... 26
Figure 20 Temperature and flow variation during the heat up transient [18] 27
Figure 21 Temperature and flow variation during the heat up transient [20] 27
Figure 22 Temperature differences between top and bottom inner wall surfaces [20] 28
Figure 23 Temperature differences between top and bottom wall surfaces [20]..... 28
Figure 24 Temperature differences between top and bottom wall surfaces [22]..... 29
Figure 25 Pressurizer surge line model of CHASNUPP II [23] 30
Figure 26 Pressurizer surge line model [24] 30
Figure 27 Pressurizer surge line geometric configuration and layout..... 47
Figure 28 Pressurizer surge line monitoring points and cross sections..... 48
Figure 29 Pressurizer surge line meshing in ICEM 49
Figure 30Top to bottom temperature difference for heat up rate of 30 gpm [2]..... 2
Figure 31 Pressurizer surge line monitoring points and cross sections..... 6
Figure 32 and bottom inner wall surface temperature difference at flow velocity of 0.05 m/s 7
Figure 33 Top and bottom outer wall surface temperature difference at flow velocity of 0.05 m/s..... 8
Figure 34 TIS and BIS for k-ε model at flow velocity of 0.05 m/s plane 1 9
Figure 35 TOS and BOS for k-ε model at flow velocity of 0.05 m/s plane 1 9
Figure 36 TIS and BIS for RNG k-ε model at flow velocity of 0.05 m/s plane 1 10
Figure 37 TOS and BOS for RNG k-ε model at flow velocity of 0.05 m/s plane 1 .. 10
Figure 38 TIS and BIS for SST model at flow velocity of 0.05 m/s plane 1 11

Figure 39 TOS and BOS for SST model at flow velocity of 0.05 m/s plane 1 11
Figure 40 Inner wall surfaces temperature differences for 3 flow velocities at plane 2 13
Figure 41 Outer wall surfaces temperature differences for 3 flow velocities at plane 2 14
Figure 42 TIS and BIS for SST model at flow velocity of 0.05 m/s plane 2 15
Figure 43TOS and BOS for SST model at flow velocity of 0.05 m/s plane 2 15
Figure 44 TIS and BIS for SST model at flow velocity of 0.1 m/s plane 2 16
Figure 45 TOS and BOS for SST model at flow velocity of 0.1 m/s plane 2 16
Figure 46 TIS and BIS for SST model at flow velocity of 0.2 m/s plane 2 17
Figure 47 Pressurizer surge line model with downward slope of five degree 19
Figure 48 top to bottom inner wall surface of pressurizer surge line model with an overall slope of 5 degree 20
Figure 49 TIS for different cross sections with over all downward slope of 5 degree 21
Figure 50 BIS for different cross sections with over all downward slope of 5 degree 21

List of Tables

Table 1 Worldwide Nuclear Reactor types 2016 [7]..... III
Table 2 Pressurizer Surge Line Specifications..... 5
Table 3 List of Nuclear Power Plants reported Cracking Indications..... 10
Table 4 Causes of Cracking in Feed Water Line 11
Table 5Temperature with respect to element numbers 51
Table 6 Comparison of simulation constraints..... 52
Table 7 Paremetric Values 5
Table 8 Three models inner and outer surfaces temperature differences at 200s for plane 1 12
Table 9 Time span of temperature difference curves for inner wall surfaces at plane 2 14

List of Conference Papers

Second International Conference on Energy Systems for Sustainable Development (ESSD) February 21-23, 2018 "A study of thermal stratification for pressurizer surge line with different turbulence models and flow velocities"(Presented as first author)

Second International Conference on Energy Systems for Sustainable Development (ESSD) February 21-23, 2018 "To study over all downward slope of pressurizer line for thermal stratification"(Presented as first author)

International Conference on Effect of Nanotechnologies on Energy (Nano-SET) 25-27 October 2017 "Effect of heat transfer and fluid flow on entropy generation in Nano fluids" (Presented as second author)

13th International Conference on Emerging Technologies (ICET-2017) will be held in Islamabad, on 27-28 December 2017. "Numerical simulation of particulate removal efficiency in venturi scrubber" (Presented as second author)

Abstract

Pressurizer water reactor is commonly used operating nuclear power plant. Thermal stratification is common issue in almost in every PWR. Thermal stratification is formation of layer in fluid due to density difference which results in thermal and fatigue stresses. In current work thermal stratification is studied using ANSYS CFX for conjugate heat transfer analysis. Three different turbulence models have been compared to analyze the temperature trend along the pressurizer surge line. The effect of different flow velocity and over all downward slope of 5 degree is considered for stratification effect. The heat up rate affects the thermal stratification phenomenon, at very low flow velocities of the order of 0.05 m/sec the top to bottom temperature difference increases and later with increase in flow velocity this difference decreases. Overall, the increase in heat up rate reduces the tendency of thermal stratification phenomenon. The RNG K-E and SST turbulence models can be used to analyze the behavior of flow in pressurizer surge line for thermal stratification condition. The well established and most widely validated standard k-ε turbulence model does not predict well due to its moderate agreement in unconfined flows, curved boundary layers and swirling flows. The overall downward slope in the pressurizer surge line affects the flow field and reduces the maximum top to bottom temperature difference along the pressurizer surge line especially in regions near pressurizer end.

Chapter 1

Introduction

1.1 Introduction

The world sees a new change in 18th century, “Industrial Revolution”, when cultural, social and economic conditions were greatly affected by this technological advancement. The 19th century added fuel to this revolution with internal combustion engines and electrical power generation using natural resources as fuel mainly coal [1].In 20^{th} century the race is joined by many which put an upper limit to industrialization based on availability of natural resources as fuel. On 2^{nd} December 1942 Enrico Fermi and Walter Zinn created first man-made reactor, known as Chicago Pile-1, which provided a new option to all for electricity generation harnessing nuclear energy[2].

1.2 Nuclear Power Plants

The commonly known history of word “NUCLEAR” is associated with the miserable incidents of Hiroshima and Nagasaki, Japan in World War II. In late 1940s and early 1950swork on nuclear energy proceeded. Eventually on 20^{th}December 1951 [3] electricity was generated for the first time by a US nuclear reactor at EBR-In experimental station Among several types of NPPs, Pressurized Water Reactor (PWR) is most common and out of 435 NPPs 270 are PWRs. NPPs provided 10.8% of world’s electricity production in 2012 and its statistic are show in Figure 1.Mostly Pressurized Water Reactors are used around the world. Reactors type, their capacity and their numbers are given in table 1.

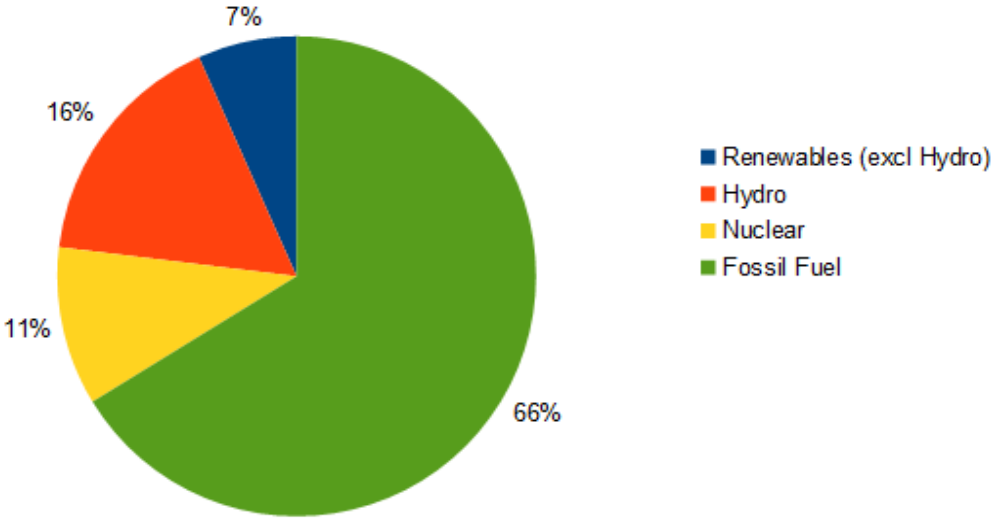

Figure 1World Electricity Consumption[6]

Table 1 Worldwide Nuclear Reactor types 2016 [7]

Types of Reactor	Numbers	Electrical net output MW
Pressurized Water Reactor(PWR)	291	272.765
Boiling Water Reactor(BWR)	78	75.208
Pressurized Heavy Water Reactor(PHWR)	49	24.634
Gas Cooled Reactor(GCR)	14	7.720
Light Water Cooled, Graphite Moderated Reactor(LWGR)	15	10.219

Fast Breeder Reactor(FBR)	3	1.369

1.2 Pressurized Water Reactor

Pressurized water reactors being the most common type of NPPs were originally designed for propulsion of nuclear submarines and later used in the original design of second commercial NPP [8]. A simple PWR consists of two coolant loops primary (pressurized water) and secondary (steam line). The steam generator exchange heat between primary and secondary coolant loop and hence, produce steam in secondary coolant loop. The secondary coolant loop directs the steam to the main turbines causing it to turn turbine generator, which generates electricity [9]. A layout of typical PWR is depicted in Figure 2.

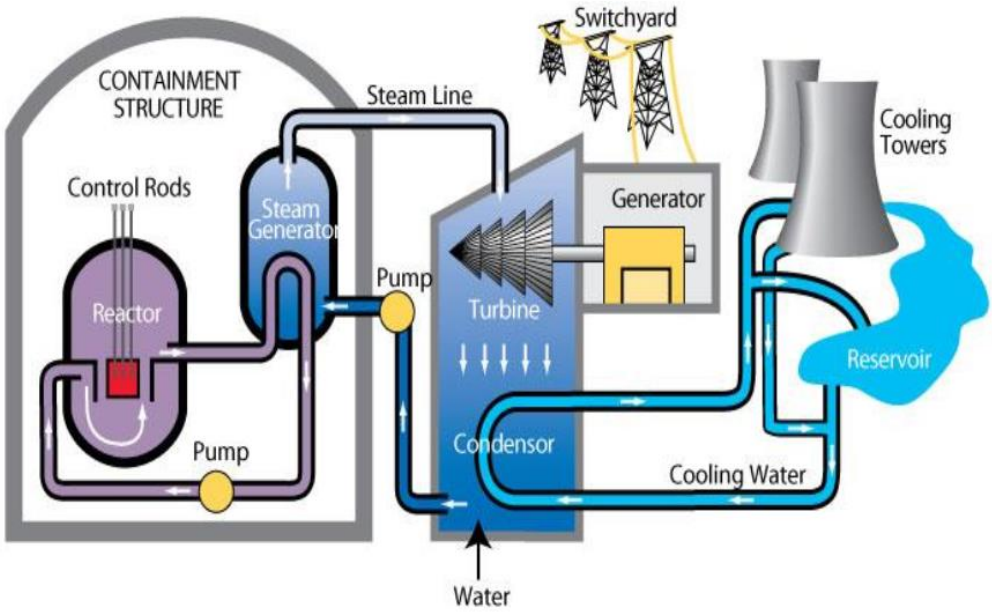

Figure 2 Layout of typical PWR [9]

The PWR is categorized among the other types of NPP by its two main characteristics.

a) Separate coolant loops (primary and secondary) for pressurized water and steam.
b) The high pressure in the primary loop.

These loops serve as barrier to radioactivity.

1.4 Pressurizer surge Line

The pressurizer is a crucial part of the main coolant loop. The pressurizer maintains the pressure inside the main coolant loop and controls for the pressure and volume surges. The pressurizer is connected to the primary coolant loop via a pipe known as pressurizer surge line depicted in Fig 3. If pressurizer surge line is subjected to any thermal load will greatly affect the structural integrity of the pipe and can hamper the operation of NPP.

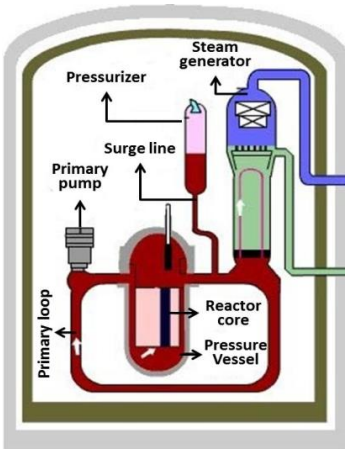

Figure 3 label diagram of typical PWR

The pressurizer surge line is typically a stainless steel type 316 pipe that facilitates the operation of pressurizer. It runs down horizontally and vertically from pressurizer end with different slopes and curvatures and joins the primary coolant loop. A design of pressurizer surge line is depicted in Fig 4.

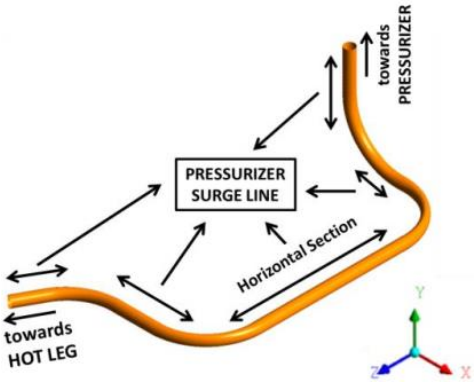

Figure 4 Typical layout of pressurizer surge

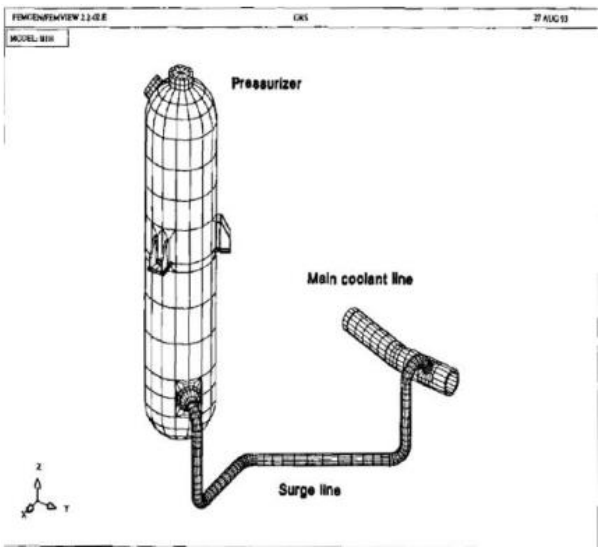

Figure 5 Surge line layout 1 [10]

Mostly the pressurizer surge line of various pressurized water reactors is similar in configuration, still they vary a little mainly due to the overall plant design requirements and piping layouts. Almost in all of the of the pressurizer surge line layouts they run down vertically from the pressurizer with few exceptions such as in German design the pressurizer surge line has a small horizontal section at pressurizer end as depicted in Fig 5.In figure 6,7,8 and 9 different layouts of pressurizer surge line are shown.

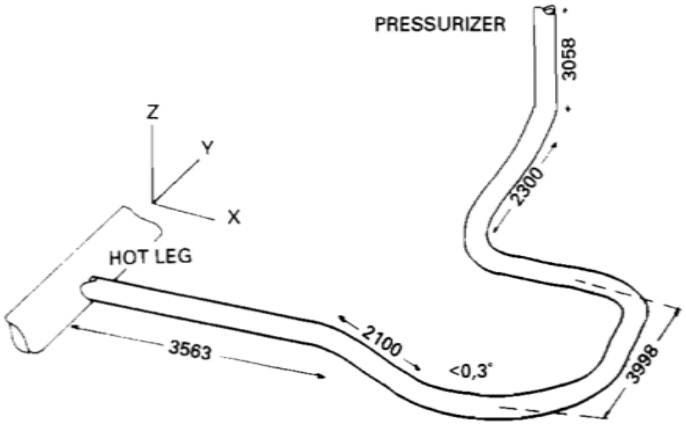

Figure 6 Surge line layout 2 [11]

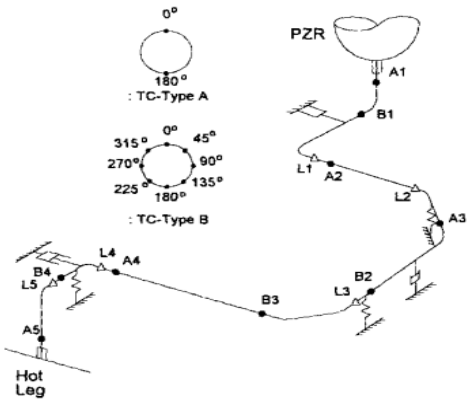

Figure 7 Surge line layout 4[13]-[14]

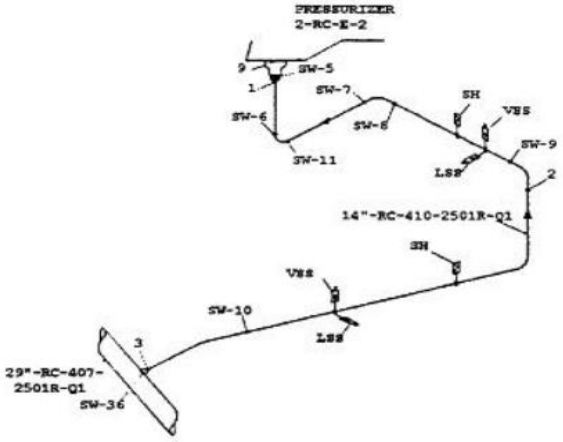

Figure 8 Surge line layout 3 [12]

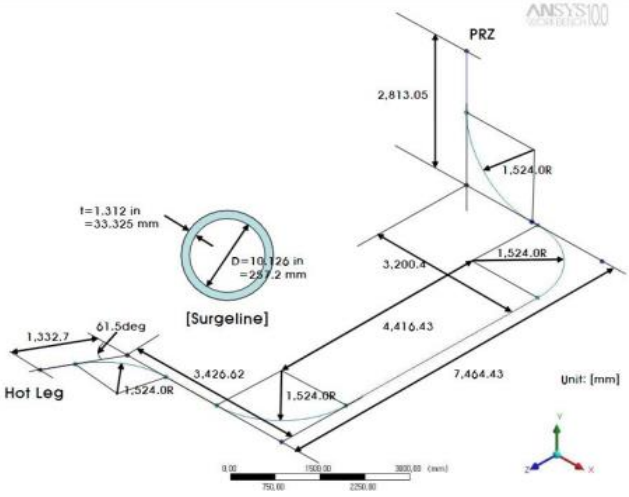

Figure 9 Surge line layout 8 [15]

The pressurizer surge line layout varies with the hot leg joining angle as depicted in above Figures. The long horizontal or near horizontal section is common in most of layouts.

The diameter of pressurizer surge line ranges from 250 to 350 mm (10 to14 inches) with thickness of 30 to 50 mm (1.2 to 2 inches) in different nuclear power plants. The overall length of pressurizer surge line is in range of 17 to 25 m (55 to 80ft). Pressurizer surge line specifications of different power plants from various countries are given in Table 2.

Table 2 Pressurizer Surge Line Specifications

S No	Country	Inner Dia mm	Thickness mm	Length M	Material
1	NPP Germany	350	40	23.8	Steel
2	NPP Germany	317	25	11	Steel
3	CRUAS 2 France	317	25	11	Steel
4	NPP USA	254- 355.6	25	11	Type 316 SS
5	Surry Unit 1 & 2 USA	266.85	28.5	11	Type 316 SS
6	North Anna Unit 1 & 2 USA	293.014	31.293	11	Type 316 SS
7	YGN 3 & 4 (Korea)	304.8	31.293	11	Type 347 SS
8	KORI Unit 1 (Korea)	257.2	33.325	16.5	Type 316 SS
9	NPP (Korea)	270	30	16.5	Type 347 SS
10	NPP (Korea)	233	36	16.5	Type 316 SS

1.5 Thermal stratification and Pressurizer surge Line

In fluids stratification is the formations of layers in such a way that hot fluid layer is followed by cold fluid layer due to different densities and temperatures. When the flow is stratified due to temperature difference the phenomena is known as thermal stratification. Stratification phenomena or stratified flow is a well-known case in high temperature applications. In thermal stratification of fluids the layer formation is caused by buoyancy effect in which fluid layer with lower density resides at top and followed by higher density layers. One of those is nuclear power plants where system works at high temperature and pressure. Pressurized water reactor (PWR) is a common example of that. One of the main concerns is the pressurizer surge line, in which hot water from the pressurizer flows over cold water layer, leading to time dependent temperature fluctuations and a risk for thermal fatigue [16].

1.6 Problem Statement

In this study pressurizer surge line of PWR is analyzed for thermal stratification. The analysis is performed through numerical simulation mainly due to two reasons, firstly it waives the high cost of experimental setup and secondly it facilitates an option to investigate diverse models.

To understand stratification in surge line of PWR requires realistic time dependent temperature distribution along the wall. The thermal hydraulic analysis to acquire the temperature distribution is performed using ANSYS CFX.

The study is performed in three phases to achieve the defined research objectives. These three phases are merely independent of each other in terms of evolution since analysis results of each phase influence the other. The three phases are enumerated below;

Phase – 1 Analysis of pressurizer surge line for different turbulence model

Phase – 2 Analysis of pressurizer surge line for different flow velocities

Phase – 3 Analysis of pressurizer surge line for over all downward slope of 5 degree.

1.7 Objectives

Thermal stratification is considered as the most important loading on pressurizer surge line. Nuclear authorities have made it a requirement to analyze thermal stratification for pressurizer surge line in the design process. The analysis of thermal stratification in pressurizer surge line can be carried out through experimentation or analyzing the online monitoring temperature data. The development of high performance supercomputers has made it possible to evaluate complex geometries such as of pressurizer surge line using commercially available CFD codes like ANSYS. Moreover a simulation study is more cost effective since different surge line models can be analyzed avoiding the huge cost involved for experimental setup. Therefore, to evaluate and analyze the thermal stratification for pressurizer surge line a CFD simulation is selected. The major dissertation objectives are enumerated as such;

1 To develop a 3-D CFD model for thermal stratification phenomenon
2 To obtain a realistic temperature distribution using a realistic 3-D model of Kori 1 Pressurizer surge line
3 To analyze different turbulence models for thermal stratification
4 To analyze different flow variation of pressurizer surge line under thermal stratification
5 To study over all downward slope of 5 degree for pressurizer surge line thermal stratification

1.8 Outline of Thesis

The content of this thesis is divided into five chapters. The brief details of each chapter contents are listed below.

Chapter 1: Introduction

This chapter describes the importance of pressurizer surge line for a PWR. This chapter also describes the objective of this study. In the end, Flow chart of thesis is described.

Chapter 2: Literature Review

This chapter describes the previously conducted experimental and numerical work for pressurizer surge line thermal stratification. The observations of previous work have also been described briefly in this chapter.

Chapter 3: Numerical Modeling

This chapter describes the details of turbulence models, momentum transfer model, Reynolds averaged Navier-Stokes and energy equation which have been used in this research.

Chapter 4: Chapter 4 CFD Analysis Verification and Validation

This chapter describes the details of pressurizer surge line geometry, unstructured grids, and model validation.

Chapter 5: CFD Analysis

The CFD results of pressurizer surge line have been analyzed in this chapter. The effect of flow velocity, choice of turbulence model and over all downward slopes is analyzed for pressurizer surge line in this chapter.

1.9 Summary

The requirement of energy is growing every day with new inventions and pursuit for better life. Nuclear power plants have been considered as electricity source for all developed or developing countries. Thus, over 400 nuclear power plants are providing electricity around the world. Among different types of nuclear power

plants pressurized water reactor are most common. Pressurizer is a key component of pressurized water reactor which facilitates the pressure and volume surges and maintains pressure inside the primary coolant loop. Any damage to the integrity of pressurizer surge line will hamper the operation of nuclear power plant.

Chapter 2

Literature Review

2.1 History of Thermal stratification

The thermal stratification phenomena lead us back to three decades, when in 1979, USNRC (U.S. Nuclear Regulatory Commission) issued Bulletin No 79-13 on notification of Indiana and Michigan Power Company about the cracking in two feed water lines at their D. C. Cook Unit 2 facility[1].

2.1.1 D.C. Cook Power Plant-Feed Water Lines

Donald C. Cook Power Plant is in the town of Bridgman, Michigan, USA. It is a PWR with capacity of 1090 MW. The cracking at D.C. Cook Unit 2 facility discovered on May 19, 1979 to investigate leakage inside containment. On May 25, 1979 [1], Office of Nuclear Reactor Regulation informed all licensees about the D. C. Cook failures and requested specific information on feed water system design, fabrication, inspection and operating histories. Upon requested inspections, similar cracking indications in feed water nozzle to piping welds were observed and reported on facilities listed in Table 3.

Table 3 List of Nuclear Power Plants reported Cracking Indications

Date	Location	Reported by
June 05, 1979	San Onofre Unit 1	Southern California Edison
June 15, 1979	H. B. Robinson Unit 2	Carolina Power and Light
June 18, 1979	Beaver Valley Unit 1	Duquesne Power and Light
June 20, 1979	Salem Unit 1	Public Service Electric and Gas Company

The extensive investigations were carried out by Westinghouse and determined causes are listed in Table 4.

Table 4 Causes of Cracking in Feed Water Line

Location	Cause of Failure
D. C. Cook Units 1 and 2	fatigue assisted by corrosion
San Onofre Unit 1	stress assisted corrosion

However, it was established that the cracking experienced at both of the above facilities appear to have different cause - effect relationships, and furthermore it was stated that the phenomena could not be fully understood at that time [1].

2.1.2 Farley 2 and Tihange Power Plant - Leakage in RCS to Unisolable Piping

The Joseph M. Farley Power Plant is situated near Dothan, Alabama, USA. Farley 2 is PWR with capacity of 920 MW. On December 9, 1987 at Farley 2 an unidentified leakage of 0.7 gallons per minute (gpm) from reactor coolant system (RCS) to emergency core cooling system (ECCS) was determined. The temperature stratification occurred in the ECCS system as temperature fluctuations at location of failed weld were found to be as large as 72 °F and with varying periods between 3 to 22 minutes. The Tihange Nuclear Power Plant is located in Belgian district of Tihange, Belgium. It is a PWR with capacity of 962 MW [2]. Similar incident was reported in a foreign reactor on June 6, 1988, when an abnormally high flow rate of 0.2 gpm to the containment sump was detected [2]. In the three incidents leakages to the un-isolable piping which is connected to the RCS resulted in cracking due to the temperature stratification. Since the temperature in the RCS is higher than the un-isolable piping. However, for these power plants the effects of thermal stratification were not considered in the piping design.

2.1.3 Torjan Power Plant - Pressurizer surge Line

On October 7, 1988 the staff of the Torjan Power Plant issued an Information Notice 88-80, which states that the plant has observed unpredicted movement of the pressurizer surge line at every refueling since 1982 [3],[4]. The monitoring program was implemented upon the removal of the thermal sleeve. The Trojan report indicated that thermal stratification might have occurred in the pressurizer surge line during heat up, cool down, and steady-state operation of the plant.

2.1.4 French Reactors – PWR Surge Line

The temperature monitoring of different French reactors (PWR) is being done since 1981 [5]. Later in years to come with further increase in monitoring and subsequent research established that the phenomenon was common to all 900 MW French PWR.

2.1.5 Dampierre 4 Nuclear Power Plant - 1st Observation

The Dampierre 4 PWR is located in the town of Dampierre-en-Burly (Loiret), France. The stratification was observed in surge line and it was the first monitored observation. Stratification occurred on the horizontal section and under low flow rates [20].

2.1.6 Cruas 2 Nuclear Power Plant - Stratification in Horizontal Section

The Cruas 2 PWR is located in Cruas, France. It is a three loop 900 MW unit. In 1984 [20], a temperature monitoring program was conducted on the pressurizer surge line of Cruas 2. The results showed that stratification takes place in the horizontal section and horizontal nozzle on hot leg during steady state operation. Further it confirmed the observation made at Dampierre 4 PWR.

2.1.7 Loviisa Power Plant – Crack in Surge line

The Loviisa PWR is located in Loviisa, Finland. It is a Soviet design PWR. In 1994 a penetrating crack in the pressurizer surge line was reported. The important factor to be noted was that the stratification effects were not considered in the design basis and consequently its significance was not known at the time of construction. However the reason for the crack was established to be stratification. The pressurizer surge line thermal stratification incidents are discussed in detail and following key points are extracted;

- Thermal stratification is observed in many countries, mainly US and France, operating PWR type NPPs.
- Thermal stratification is identified as a concern that may affect the structural integrity of reactor coolant system in NPPs.
- The pressurizer surge line integrity is required to be assessed under thermal stratification condition.

2.2 Requirements of Nuclear Authorities

The pressurizer surge contains high temperature, high pressure and high radioactive reactor coolant and hence falls in the category of nuclear class I and seismic category I piping [7]. The US NRC Bulletin 88-08 [2] and 88-11 [4] specifies the acceptable actions to address the thermally stratified flow in PWR surge line and the US NRC standard review plan SRP 3.9.3 [8] provides the related rules. The actions requested by US NRC bulletin mentioned above are summarized as;

- A visual inspection of the entire pressurizer surge line including piping is to be conducted as per ASME, Section XI, VT-3 for any structural damage.

- The pressure increase line complies with applicable design codes andtaking into account the phenomenon of thermal partitioning and thermal stress in the assessment of stress.
- To obtain plant specific data of pressurizer surge line for thermal stratification either by instruments to monitor the pressurizer surge line temperature distribution and thermal movements or through collective efforts from other NPPs with similar pressurizer surge line design.

2.3 Thermal Stratification Research and Measurements

Almost two decades have passed since the USNRC threatened the Integrity of the pressure compensation line by thermal stratification [3], [4]. Several Researchers, scientists, engineers and researchers have made efforts to understand the thermal stratification phenomenon in the pressure balance to obtain temperature distributions, thermal stresses and fatigue through laboratory tests of specific geometry, field measurements.

2.3.1 US NPPs

Diablo Canyon established a program to monitor and collect the pressurizer surge line temperature profile and pipe displacement data. The resistance temperature detectors (RTDs), horizontal and vertical potentiometer were installed at four locations along the pressurizer surge line. At each of these locations five RTDs were placed around the outside surface of the pressurizer surge line at angles of 90°, 30° ,0° -30° and -90°, where 90° is the top of pressurizer surge line and data was recorded at one minute interval. The temperatures monitored at different locations are depicted in Fig 10. Hirschberg and Antaki in 1989 [9] analyzed the Diablo Canyon data and found that the thermal stratification is definitely occurring during heat up and 100% power operation with maximum top to bottom temperature gradient of 214°F (101°C) with measured maximum bow of 1.9 inches (4.826 cm) downward. They recommended that the pressurizer surge line design should be updated to incorporate the effects of thermal stratification. San Onofre nuclear

generating stations established a program to monitor the pressurizer surge line. The temporary thermocouples were installed on pressurizer surge line at locations near hot leg (point 2) and pressurizer (point 5).

Data was recorded for heat on August 8, 1988, as shown in Figure 11. Analysis of Griesbach and other [10] 10 hours full data I found a temperature prone pressure increase line Because the leg temperature has stayed hot at about 325 degrees Fahrenheit (162 ° C) while maintaining significant temperature fluctuations between pressurizer and the hot leg.In addition, you have found that the extent to which the thermal layers are developed or cleaned at various locations along the tube depends on the size and duration of the insurges/outsurgesthat causes these effects and the prevailing temperature difference between the pressurizer and hot leg..

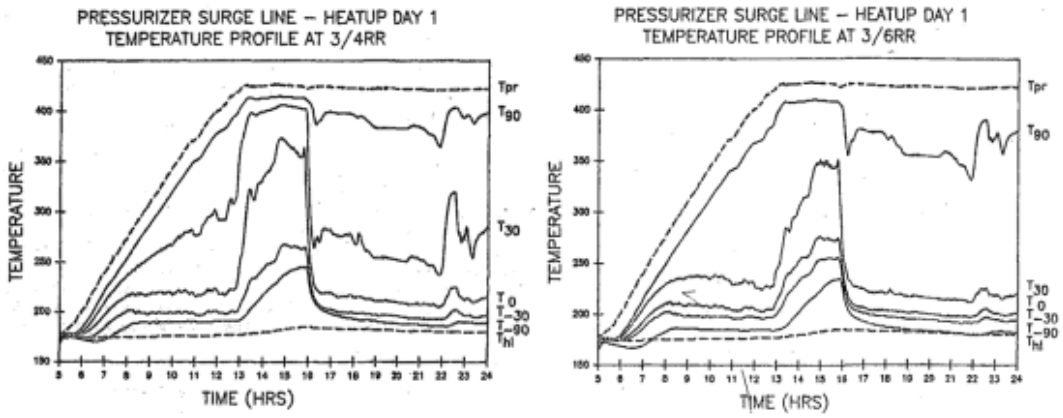

Figure 10 Transient Temperature Profile of Diablo Canyon Surge Line [9]

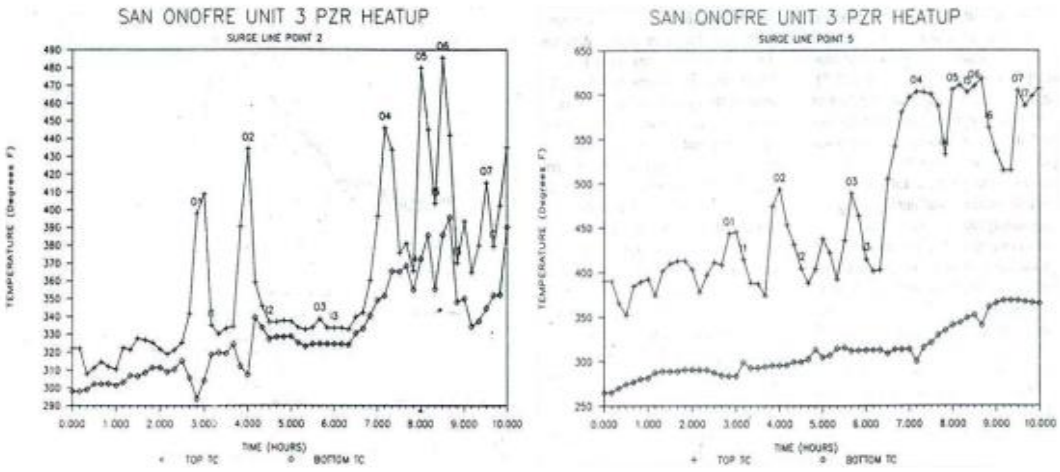

Figure 11 Transient Temperature Profile of San Onfore Surge Line [10]

2.3.2 French NPPS

FRAMATOME conducted pressurizer surge line monitoring programs at different NPPs in France [5]. They have observed thermal stratification in the horizontal section of DAMPIERE 4 pressurizer surge line in 1981 and similar observations were recorded at the horizontal section of pressurizer surge line and horizontal nozzle of pressurizer surge line on the hot leg of CRAUS 2 in 1984. However an interesting observation is made in 1986 reduced thermal stratification effects were recorded on the pressurizer surge line of CATTENOM 1 whose pressurizer surge line joins the hot leg with a 45° slope unlike other pressurizer surge line layouts generally having zero slope [10].

2.3.3 Korean NPPs

Nuclear power plant (YGN) 3 and 4 were in the design phase [11] when USRNC specified the pressurizer surge line thermal stratification requirements [2],[4]. Pressurizer surge line temperature and displacements were measured and recorded during YGN 3 pre-core hot functional test for heat up and cool down process. The measurements for heat up rates were recorded every two minutes when plant temperature changes were accepted and at every two minutes during entire

cool down process. The top to bottom temperature differential at location A3 is depicted in Fig 12.

Yu et al [6], [7] found that all temperature differences in the pressure-increasing line are associated with a change in the pressure level, i.e., a sudden increase or increase in pressure. In addition, the temperature at the lower end of the boom line remained constant and close to the hot leg temperature. In the case of heights, the temperature differences between the upper and lower edges of the rising line during the temperature rise and the cooling in the height tend. The sudden increase during cooling has led to a faster temperature reduction on the ground compared to the upper part of the increase in the line. In addition, the temperature at the top remained close to the temperature of the pressure.

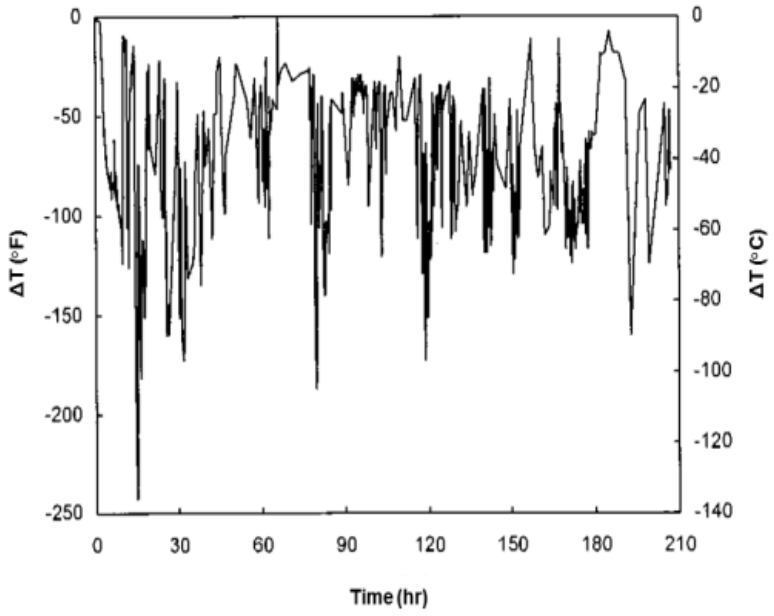

Figure 12 Top to bottom temperature difference during heat up [10]

2.4 Theoretical Prediction

Stratification in fluids is observed when there is a difference in density. In high temperature thermal hydraulic applications this density difference is caused by the

temperature difference. The fluid at higher temperature being lighter tends to flow in the upper region of pipe over fluid at lower temperature relatively at higher density causing flow to be thermally stratified. One of the high temperature applications is nuclear power plants and the pressurizer surge line is most suspected to stratification. The crucial loading on the pressurizer surge line considered by IAEA [2] is imposed by thermal stratification.

The data recorded by temperature monitoring programs and series of test revealed that temperature profile in the cross section of stratified flow can be correlated to Froude Number or the potential of stratification can be assessed by Richardson number [9].

2.4.1 Froude Number

Froude number (*Fr*) relates the velocity and buoyancy head in fluid flow applications and is given by Eq. 2.1 [13].

$$FroudeNumber = \frac{Inertail\ Forces}{Gravity\ Forces}\ or\ \frac{Velocity\ Head}{Bouyancy\ Head} \qquad (2.1\ a)$$

$$Fr = \frac{V}{\sqrt{gy_h}} \qquad (2.1\ b)$$

Where, V is fluid velocity, g is acceleration due to gravity, and $y_h$is hydraulic depth defined as in Eq. 2.2,

$$y_h = \frac{A}{W_s} \qquad (2.2)$$

Where A is the cross section of the flow section and *Ws* is the width of the water surface. The buoyancy head is related to the temperature difference between the two regions. Ensel et al.Definition of the number of Froude in relation to the intensity difference for the pressure increase-line Indicated in the Eq. 2.3 [2],

$$Fr = \frac{V}{\sqrt{gD_i \Delta\rho/\rho}} \qquad (2.3)$$

Where, V is fluid velocity, D_i = internal diameter, ρ = fluid density, and $\Delta\rho/\rho$ is defined in Eq. 2.4,

$$\Delta\rho/\rho = 2\frac{\rho_{HL} - \rho_{PZR}}{\rho_{HL} + \rho_{PZR}} \qquad (2.4)$$

Where, $\rho_{HL}$is fluid density at hot leg temperature and $\rho_{PZR}$is fluid density at pressurizer temperature.

Based on the number of Froude can be associated that occurs when the thermal splitting of the liquid in the pressure increase line

• Flow rate at burst or low sudden rise and fall

• The temperature difference between the pump and the hot leg.

That corresponds to a small Froude number. The thermal division of the line is likely to be done by pressure.

• Speed flow on rush or high

• The temperature difference between the pump and the little hot leg

This corresponds to a big Froude attitude. Therefore, the possibility of thermal partitioning when heating and cooling is greater, since the difference between the pressure and the heat velocity of the hot leg is greater.

2.4.2 Richardson Number

Number Richardson (RI) is the ratio of buoyancy force to inertia force and shows the importance of natural convection for the forced thermal load. it is defined by Grashof Number (GR) to a square of Reynolds Number (Re), such as indicated in the Eq. 2.5

$$Ri = \frac{Gr}{Re^2} \qquad (2.5)$$

Role played by Reynolds Figures Game in forced convection by Grashof number in natural convection. As such, the Reynolds number provides the main criterion in determining whether the liquid flow is one side or a turbulent one in forced convection. Similarly, the grassroot number provides the same standard of fluid flow in nature thermal load [29]. The numbers Grashof and Reynolds are in Eq. 2.6 and Eq. 2.7

$$Gr = \frac{g\beta D_i \Delta T}{\nu^2} \qquad (2.6)$$

$$Re = \frac{VD_i}{\nu} \qquad (2.7)$$

Substituting the *Gr* value from Eq. 2.5 and *Re* value from Eq. 2.6 in Eq. 2.5 we get *Ri* as given in Eq. 2.8 below,

$$Ri = \frac{g\beta D\Delta T}{V^2} \qquad (2.8)$$

If *Ri* << 1 natural convection effects are negligible, forced convection effects are negligible for *Ri* >> 1 and both effects are significant if *Ri* < 1.

Hirschberg et al. [24] has used Richardson number to assess the potential of thermal stratification in pressurizer surge line by analyzing the recorded temperature distribution. They discussed Richardson number greater than unity generally results in stratification.

2.5 Numerical Analysis and Simulations

The high cost of experimental setup and man power has made numerical analysis and simulation a beneficial tool capitalized by many researchers and scientist to assess the stratification problem. The advent of parallel processing and high computational power has made it easier to analyze complex geometries such as of pressurizer surge line using commercial codes for example ANSYS.

Taupin et al. [5] (1989), to avoid a costly three dimensional computation at that time, developed and implemented 2D/1D technique using FRAMATOME SYSTUS computer code to assess the mechanical effects of stratification in piping (pressurizer surge line). They performed calculations heat up case keeping top of pressurizer surge line at pressurizer temperature of 218°C and bottom at hot leg temperature of 51°C. A similar calculation is performed without stratification keeping the pressurizer surge line at 51°C for comparison of displacements. They found large displacement (4.04 inch) with stratification loads as depicted in Figure 13. A displacement of 1.28 inch is found without stratification. They also found that

temperature fluctuation amplitude is too low and temperature fluctuations were too quick to affect the pressurizer surge line. Thus, thermal stripping is a negligible phenomenon.

They discussed that avoiding stratification by process modifications requires a highflow rate that is difficult to achieve and recommended alternative design solutionsthat could reduce stratification effects, such as;

a) increasing the pressurizer surge line overall slope

b) Inserting a vertical pipe section immediately ahead of the hot leg

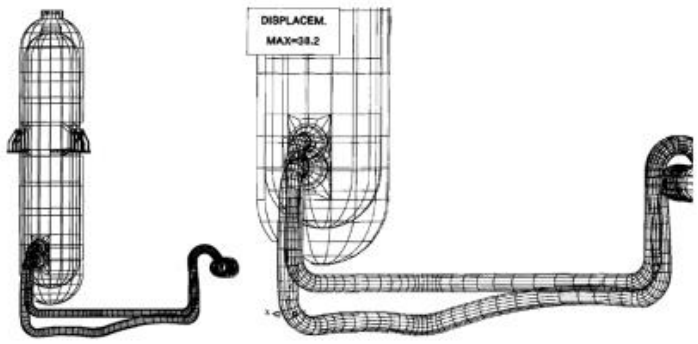

Figure 13 Deformation of complete solid element model [1]

H. Grebner et al. [1] in 1995 investigated the stratification effects on the pressurizer surge line of PWR during start up procedure using ADINA finite element analysis software on the basis of temperature measurements at German PWR indicating thermal stratification of pressurizer surge line. They used pipe elements for easy generation of model, and less number of unknown degree of freedom. The 3D solid elements are used for detailed study of stratification effects.

The pipe element analysis is performed using mean values of temperature distribution as depicted in Figure 14.

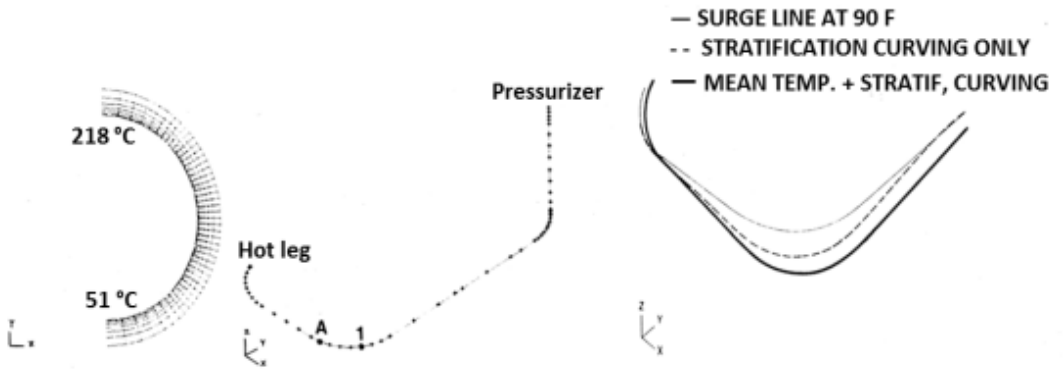

Figure 14 Pressurizer Surge Line Model (Left) and Deformation (Right) [5]

The calculation with 3D solid element models are performed using detailed temperature distribution as depicted in Fig. 15.

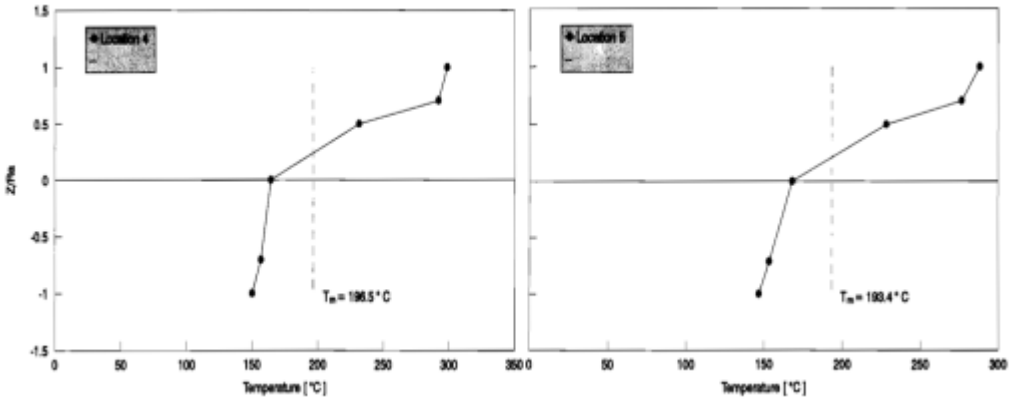

Figure 15 Temperature Distribution in Pressurizer Surge Line Cross Section [1]

Yu et al. in 1995 performed finite element analysis to predict the pressurizer surge line wall temperature distributions using and 8-node planar bi-quadrilateral element [2] as depicted in Fig. 1.21.

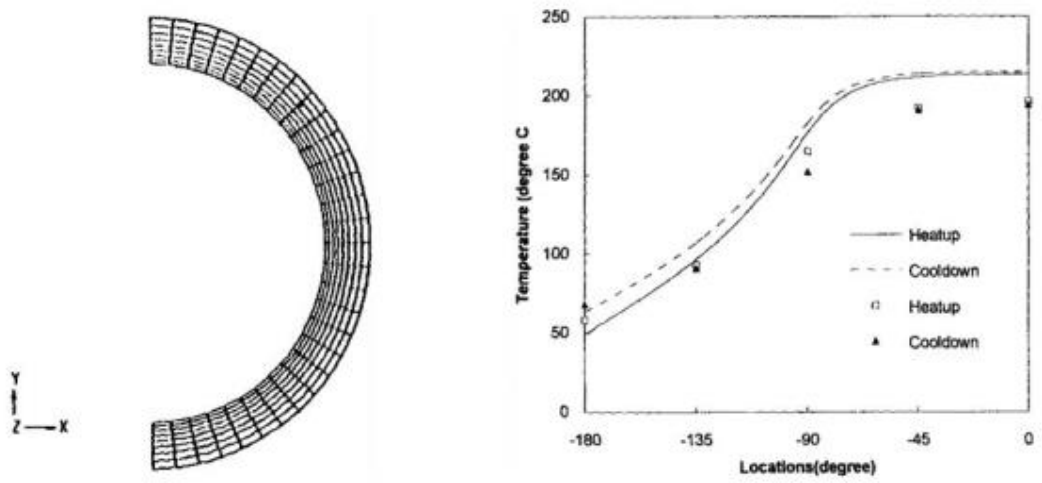

Figure 16 Finite Element Model and Comparison of Circumferential Temperature [3]

The predicted temperatures were in good agreement with the measured values a comparison plot circumferential temperature distribution is depicted in Figure 16. The pressurizer surge line was modeled with the CEMARC computer code for finite element analysis.

Jeong et al. in 1999 presented a method to mitigate thermal stratification of a horizontal long pipeline in a circular cylinder by heating the external bottom surface of the cylinder with electrical heat tracing [15]. They developed an unsteady two-dimensional numerical analysis model and computer program to investigate the effect of external heating on thermal stratification. An outsurge case during power plant heat up operation was analyzed. The pipe was heated externally at bottom by heat tracing. They found that stratification could be diminished. The external heating mixes the hot and cold water 25 % earlier from the case without heating, whereas, the maximum dimensionless temperature difference of the pipe inner wall is reduced 17.1 % from 0.514 to 0.424 and that of fluid is reduced to 22.5 % from 0.449 to 0.348 as depicted in Figure 17.

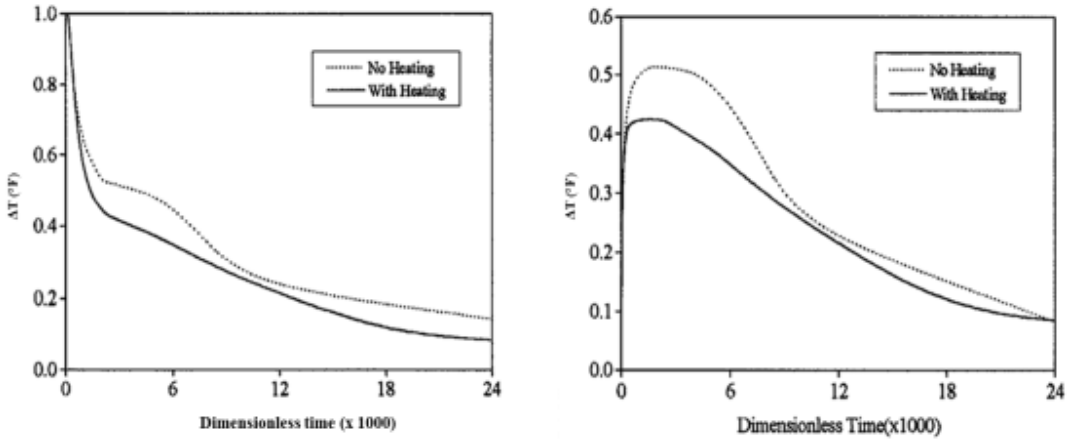

Figure 17 Comparison of Temperature Difference Change between No Heating and External [15]

Jo et al. in 2001, presented a way to simulate a thermal stratification in Circular tube and prediction of the distribution of the transient temperature in the tube wall withNumerical analysis [16]. They examined three different fluid levels in diameter ID 0.25, ID 0.5, and 0.75 ID (ID = inside diameter). The temperature drops from top to bottom in the peripheral direction and the temperature is independent of the interface level if it is equal to or more than 0.5 ID.

Jo et al. in 2003 carried out a detailed numerical analysis of the unstable function. heat transfer and thermal pressure for the flow-line model of a PWR.Thermal stratification caused by an increase in the mutant flux considering the thickness of the pipe wall [16]. The flow was thermally stratified in the tubes simulated with the k-ε model. They solved only half the solution scope provided they are thermally and geometrically similar. They also recommended that for strong design and safe and reliable safety for PWR Pressure pipe system to increase the distribution of the transient temperature in the pipe.

Boros and Aszodi in 2008 simulated the stratified flow in the pressurizer surge line and the injection line of high pressure injection system of VVER-440 reactor using CFX code [17]. The surge line model and mesh are depicted in Fig 18.

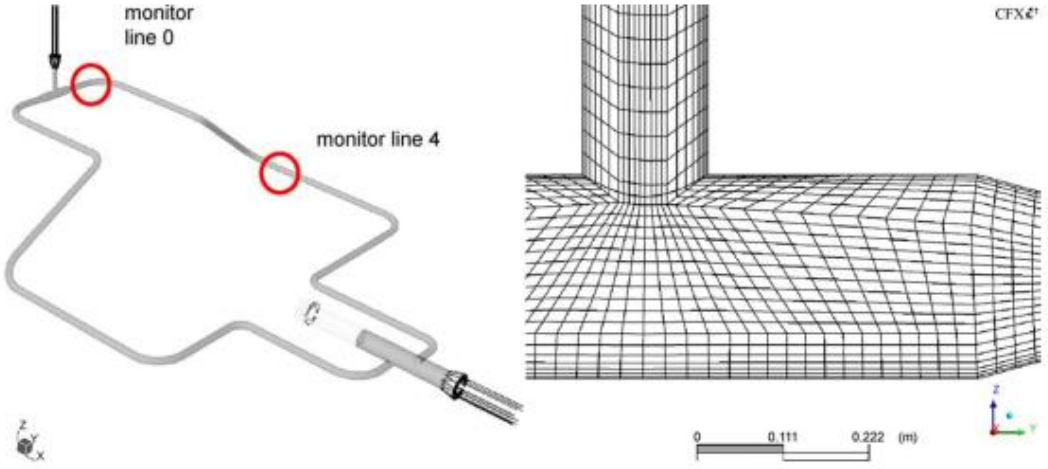

Figure 18 Pressurizer surge line model of VVER-440 and meshed T-Junction [17]

The heating stage is simulated. The simulation results match well with temperature measurement.

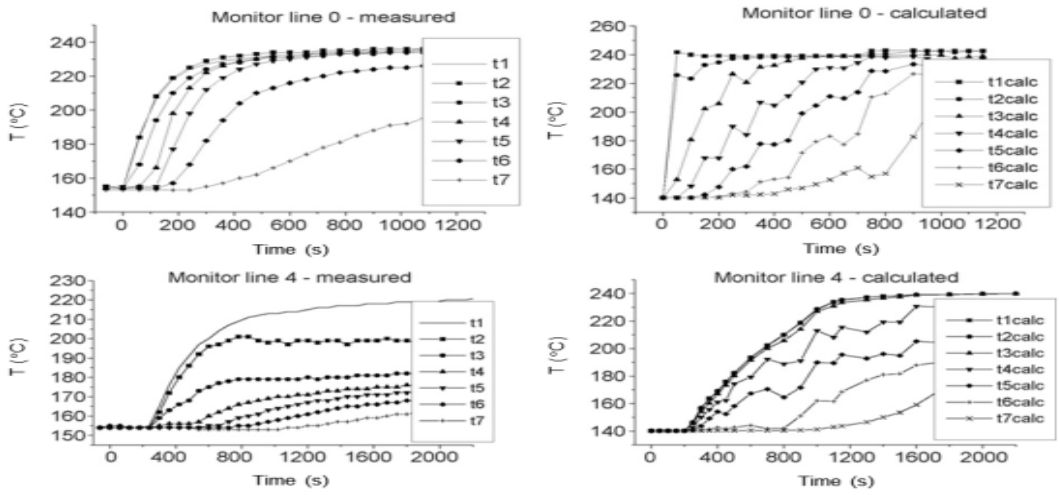

Figure 19 Measured and calculated coolant temperatures in the pressurizer surge line at monitor line 0 and 4 [17]

Kim et al. in 2008 studied the effect of vertical pipe length on the thermal stratification in the pressurizer surge line [18]. The study was performed for full three dimensional transient fluid solid interaction (FSI) analyses with FLUENT code. The heat up phase as depicted in Fig 20 was chosen for the time transient analysis with total 27000 seconds transient time.

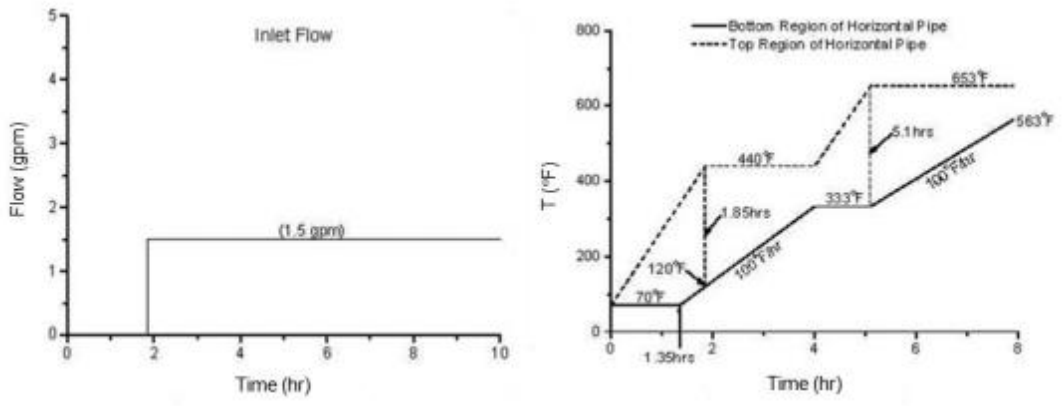

Figure 20 Temperature and flow variation during the heat up transient [18]

Jo et al. in 2008 performed a CFD analysis of thermally stratified flow and heat transfer in actual PWR pressurizer surge line of Kori Unit 1 using ANSYS CFX [19]. The geometrical model configuration and dimensions are depicted in Fig 21.

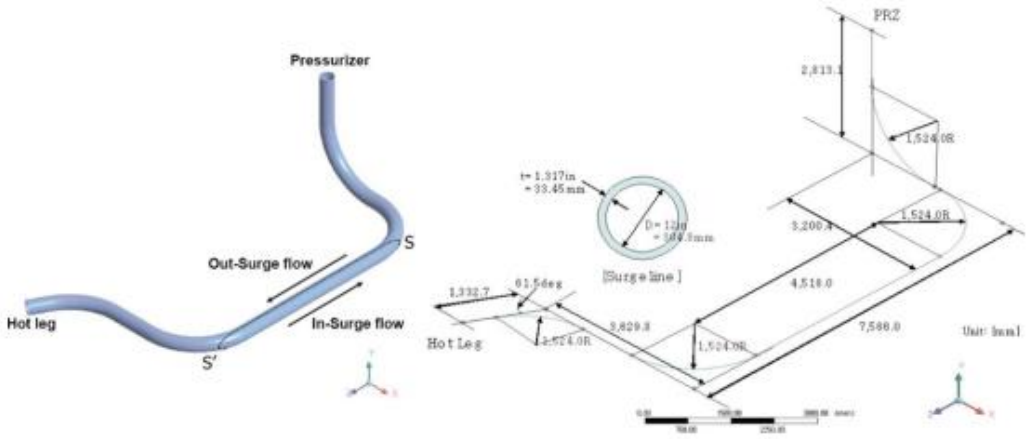

Figure 21 Temperature and flow variation during the heat up transient [20]

For out surge case the cold water initially present in the pressurizer surge line and hot water is considered to surge out of pressurizer. They found that the wall temperature predicted from simple heat transfer model not considering the pipe wall thickness as shown in Fig 22.

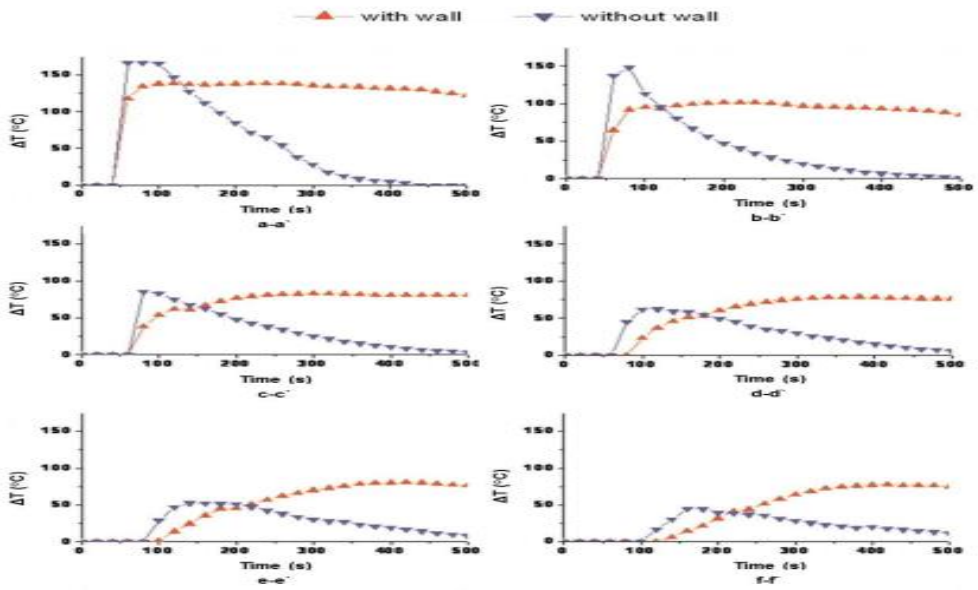

Figure 22 Temperature differences between top and bottom inner wall surfaces [20]

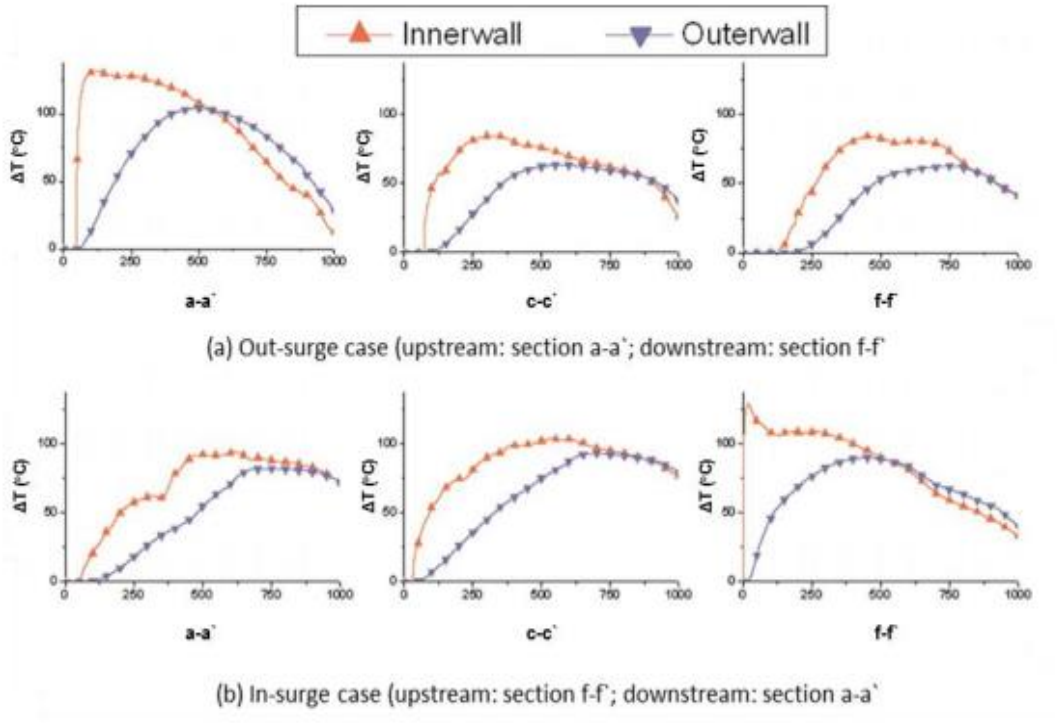

Figure 23 Temperature differences between top and bottom wall surfaces [20]

Korea Institute of nuclear safety (KINS) in 2009 performed a fluid solid interaction simulation in ANSYS environment to assess the thermal stratification in the pressurizer surge line [21]. The study concluded that the stress deviation from the mutational state is almost the same as that resulting from the sudden increase case.

Kim et al. in 2009 discussed the effect of heat up transient condition and excessive conservativeness of 2D finite element model for pressurizer surge line thermal stratification [22].

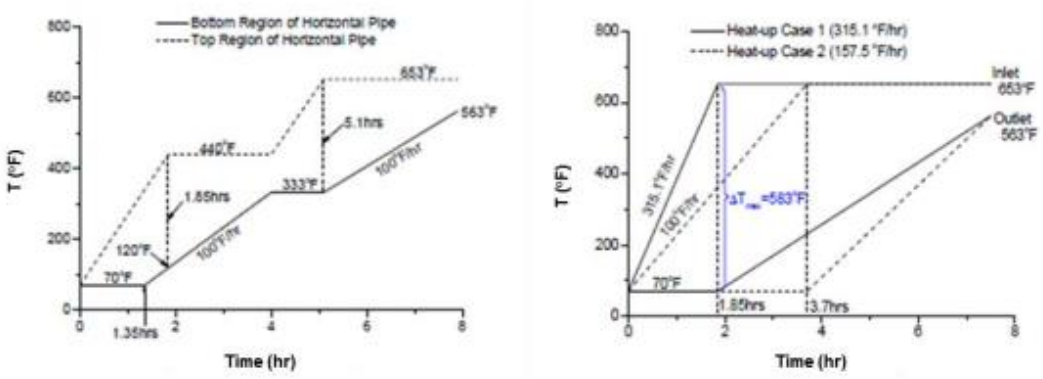

Figure 24 Temperature differences between top and bottom wall surfaces [22]

They concluded that as the flow rate increased, the temperature rose. Generally rising as the heating rate is increased; increase in the difference in maximum temperature is increased in the same place.

Asfand in 2010 performed CFD analysis to evaluate the temperature distribution in pressurizer surge line of CHASNUPP Unit II using FLUENT a commercial CFD code for reactor full power mode [23]. He found that the thermal stratification does not propagate along the whole length of pressurizer surge line and is only observed in a very short length. He mentioned that the 22.5° bend at the hot leg end of pressurizer surge line significantly reduces thermal stratification.

Figure 25 Pressurizer surge line model of CHASNUPP II [23]

Qi and Cao in 2010 studied surge line thermal stratification using numerical simulation method during reactor heat up [24]. They conducted the 3D thermal hydraulic and mechanical analysis. The pressurizer surge line is sloped about 30° from horizontal towards the hot leg end. As depicted in Fig 26. The turbulent behavior of fluid flow was simulated with SST turbulence model. The fluid properties are calculated by IPAWS-97 formulation. The results of thermal hydraulic analysis are transferred as input for mechanical analysis. The pressurizer surge line is constrained at both ends for all displacements. They observed that the top to bottom temperature difference can exceed 50K and high stress level at the bottom and around the thermal stratification interface.

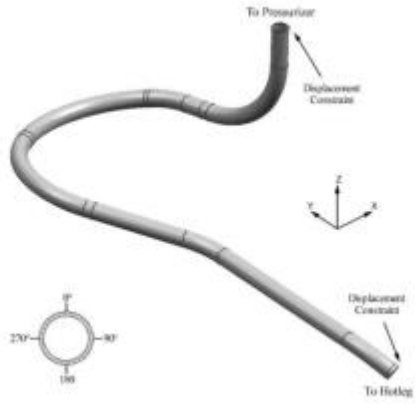

Figure 26 Pressurizer surge line model [24]

2.6 Literature Review Findings

The major research conducted on pressurizer surge line thermal stratification has been briefly introduced in preceding text and following findings has been deduced;

(a) Thermal stratification in PWR pressurizer surge line is a known phenomenon which has been observed and reported in many countries. The pressurizer surge line geometry and layout play an important role in mitigating the thermal stratification effects.

(b) The reported measurements indicate that calculated temperature difference during heat up and cool down is similar. Outsurges during heat up result in substantial temperature gradients, ranging from 30% to 70 % of pressurizer to hot leg temperature difference. Conversely insurges reduce the top to bottom temperature gradients to near zero.

(c) A 3D model of pressurizer surge line provides more realistic thermal hydraulic analysis since the temperature profile at any cross section of pressurizer surge line length is not 100 % symmetrical.

2.7 Summary

Thermal stratification phenomenon may impose a threat to the integrity of pressurizer surge line and same has been reported in history. The development of high performance supercomputers has made it possible to evaluate complex geometries such as of pressurizer surge line using commercially available CFD codes like ANSYS avoiding high cost of experimental setup and facilitating the option to analyze different models.

Chapter 3

Numerical Modeling

To analyze thermal layers in pressure increase line, a realistic temperature distribution is required. The liquid analysis is performed in ANSYS CFX to obtain the temperature distribution along the pressure increase line. To consider the analysis of the fluid structure, the associated heat transfer analysis is included in the CFD analysis.

3.1 Governing Equations

The equations governing the fluid flow are mathematical data for the laws of physics [1].

(a) The liquid mass is retained.

(b) The rate of change of dynamics corresponds to the sum of the forces on a

Liquid particle.

(c) The rate of energy transition equals the total rate of heat addition to the rate

of work performed on the liquid particles.

The three phrases above are commonly known as the Comprehensive Conservation Law, Newton's Second Law and the First Law of Thermodynamics, and the equation

derived from these laws is defined simultaneously in the name of continuity, momentum, and energy.

3.1.1 Continuity Equation

The unsteady, three-dimensional mass conservation or continuity equation for a compressible fluid is given as Eq. 3.1

$$\frac{\partial \rho}{\partial t}+\frac{\partial(\rho U_x)}{\partial x}+\frac{\partial(\rho U_y)}{\partial y}+\frac{\partial(\rho U_z)}{\partial z}=0 \qquad (3.1\ a)$$

$$\frac{\partial \rho}{\partial t}+\nabla\cdot(\rho U)=0 \qquad (3.1\ b)$$

$$\frac{\partial \rho}{\partial t}+\frac{\partial \rho U_i}{\partial x_i}=0 \qquad (3.1\ c)$$

Where, U, ρ, and ∇ refer to the velocity vector, density, and divergence operator. Eq. 3.1c is a continuity equation in the form of index.

3.1.2 Momentum Equation

Newton's second law states that the fluid dynamics exchange rate of a Particle corresponds to the sum of the forces on the particles. The forces can be as Surface and body forces. The components x, y and z become the momentum equation Indicated in the Eq. 3.2 .

$$\frac{\partial(\rho U_x)}{\partial t}+\nabla\cdot(\rho U_x U)=\frac{\partial(-p+\tau_{xx})}{\partial x}+\frac{\partial\tau_{yx}}{\partial y}+\frac{\partial\tau_{zx}}{\partial z}+S_{Mx} \qquad (3.2\ a)$$

$$\frac{\partial(\rho U_y)}{\partial t}+\nabla\cdot(\rho U_y U)=\frac{\partial\tau_{xy}}{\partial x}+\frac{\partial(-p+\tau_{yy})}{\partial y}+\frac{\partial\tau_{zy}}{\partial z}+S_{My} \qquad (3.2\ b)$$

$$\frac{\partial(\rho U_z)}{\partial t}+\nabla\cdot(\rho U_z U)=\frac{\partial\tau_{xz}}{\partial x}+\frac{\partial\tau_{yz}}{\partial y}+\frac{\partial(-p+\tau_{zz})}{\partial z}+S_{Mz} \qquad (3.2\ c)$$

Where p refers to pressure or natural pressure, τ_{ij} points to nine stress components and S_M denote the sources terminology, which includes the contribution of the body Forces.

3.1.3 Navier-Stokes Equation

ANSYS CFX solves the equation of non-static Navier-Stokes in their save models. The above momentum equation contains unknown sticky stress components. In three-dimensional flows, the local strain rate consists of a linear and volumetric strain rate. In 1979, Schlichting found that the linear deformation of the fluid contained nine stress components [2]. The three linear length deformation components and six linear distortion components are given in the Eq. 3.3 at a time becomes the volumetric deformation in Eq. 3.4 indicated.

$$S_{xx} = \frac{\partial U_x}{\partial x} \ , \ S_{yy} = \frac{\partial U_y}{\partial y} \ \text{and} \ S_{zz} = \frac{\partial U_z}{\partial z} \qquad (3.3\ a)$$

$$S_{xy} = S_{yx} = \frac{1}{2}\left(\frac{\partial U_x}{\partial y} + \frac{\partial U_y}{\partial x}\right)$$
$$S_{xz} = S_{zx} = \frac{1}{2}\left(\frac{\partial U_x}{\partial z} + \frac{\partial U_z}{\partial x}\right) \qquad (3.3\ b)$$
$$S_{yz} = S_{zy} = \frac{1}{2}\left(\frac{\partial U_y}{\partial z} + \frac{\partial U_z}{\partial y}\right)$$

$$\frac{\partial U_x}{\partial x} + \frac{\partial U_y}{\partial y} + \frac{\partial U_z}{\partial z} = \nabla \cdot U \qquad (3.4)$$

In Newtonian liquid the viscous pressure corresponds to the distortion rates. For compressible fluid three-dimensional form of newton law of viscosity contain two constants. The nine viscous stress components of which six are independent are given in Eq. 3.5.

$$\tau_{xx} = 2\mu\frac{\partial U_x}{\partial x} + \mu_2 \nabla U \qquad \tau_{xy} = \tau_{yx} = \mu\frac{\partial U_x}{\partial y} + \frac{\partial U_y}{\partial x}$$
$$\tau_{yy} = 2\mu\frac{\partial U_y}{\partial y} + \mu_2 \nabla U \qquad \tau_{xz} = \tau_{zx} = \mu\frac{\partial U_x}{\partial z} + \frac{\partial U_z}{\partial x} \qquad (3.5)$$
$$\tau_{zz} = 2\mu\frac{\partial U_z}{\partial z} + \mu_2 \nabla U \qquad \tau_{yz} = \tau_{zy} = \mu\frac{\partial U_y}{\partial z} + \frac{\partial U_z}{\partial y}$$

The replacement of the above-mentioned strains in the momentum equation leads to the Navier Stokes equation, as in Eq. 3.6.

$$\frac{\partial(\rho U_x)}{\partial t}+\nabla(\rho U_x U)=-\frac{\partial p}{\partial x}+\nabla(\mu\ grad\ U_x)+S_{Mx} \quad (3.6\,a)$$

$$\frac{\partial(\rho U_y)}{\partial t}+\nabla(\rho U_y U)=-\frac{\partial p}{\partial y}+\nabla(\mu\ grad\ U_y)+S_{My} \quad (3.6\,b)$$

$$\frac{\partial(\rho U_z)}{\partial t}+\nabla(\rho U_z U)=-\frac{\partial p}{\partial z}+\nabla(\mu\ grad\ U_z)+S_{Mz} \quad (3.6\,c)$$

3.1.4 Reynolds averaged Navier-Stokes equation

“Navier-Stokes” equations explain both volatile and unstable streams without the need for additional information. To ensure that the effects of the disease are predictable, a large amount of CFD research has focused on methods that use turbulence models. The turbulence models are specifically designed to account for the effects of interference without resorting to an undeniably fine network. The turbulence models attempt to modify the original unstable Navier Stokes equations by inserting inter-and transient amounts to produce Reynolds on average Navier-Stokes (Rans) equations. The simulation of Rans equations reduces the computational effort drastically. However, the between-process introduces additional unknown terms that contain products with variable amounts that act as extra pressure in the fluid. It is difficult to identify those terms that are termed "turbulent" or "reynolds" stress and thus become unknown. Thus, the Reynolds (Troubled) confirms the need for modeling through additional equations for known quantities.

As discussed above, the turbulence models are trying to solve the modified transport equations by inserting intermediate and fluctuating components. For example, a velocity, $U_i$may be divided into an average component, $U_i$and a time varying component $u_i$as given in Eq. 3.7.

$$U_i = \overline{U}_i + u_i \qquad (3.7)$$

The average component is given by as in Eq. 3.8.

$$\overline{U}_i = \frac{1}{\Delta t}\int_{t}^{t+\Delta t} U_i dt \qquad (3.8)$$

Referring to the large time domain in relation to turbulent fluctuations, But small in relation to the time frame in which equations are solved. Replace average quantities in the Eq. 3.6 above we get restless Reynolds on average Navier-Stokes (URANS) equation as in Eq. 3.9 indicated.

$$\frac{\partial \rho U_i}{\partial t} + \frac{\partial}{\partial x_j}\left(\rho U_i U\right) = -\frac{\partial p}{\partial x} + \frac{\partial}{\partial x_j}\left(\tau_{ij} - \rho\overline{u_i u_j}\right) + S_M \qquad (3.9)$$

Boussinesq suggested in 1877 [1] that Reynolds stress may be proportional to the average strain rate of the relationship between stress and stress levels on the flow of Newtonian fluid is given in Eq. 3.10.

$$-\rho\overline{u_i u_j} = \mu_t\left(\frac{\partial U_i}{\partial x_j} + \frac{\partial U_j}{\partial x_i}\right) - \frac{2}{3}\delta_{ij}\left(\rho k + \mu_t \frac{\partial U_k}{\partial x_k}\right) \qquad (3.10)$$

Where μt refers to turbulent viscosity, which must be typical, δ_{ij}denotes a delta-Kronecker [1], and K denotes a restless kinetic energy. Enter the concept of Reynolds stress of EQ. 2.9 we get,

$$\frac{\partial \rho U_i}{\partial t} + \frac{\partial}{\partial x_j}\left(\rho U_i U\right) = -\frac{\partial p'}{\partial x} + \frac{\partial}{\partial x_j}\left[\mu_{eff}\left(\frac{\partial U_i}{\partial x_j} + \frac{\partial U_j}{\partial x_i}\right)\right] + S_M \qquad (3.11)$$

Where S_M is the total body forces, μ_{eff} refers to an effective viscosity defined by,

$$\mu_{eff} = \mu + \mu_t \qquad (3.12)$$

and $p'$is a modified pressure, defined by,

$$p' = p + \frac{2}{3}\rho k + \frac{2}{3}\mu_{eff}\frac{\partial U_k}{\partial x_k} \qquad (3.13)$$

Last term of Eq. 3.13 is associated with velocity divergence which is neglected in

ANSYS CFX, this assumption is strictly correct only for incompressible liquid.

3.2 Turbulence Models

Eq. 3.9 to 3.13 can express fluctuating variations in functions means variables when the troubled viscosity μ_t is known. The k-ε and k-ω are two models of equation using this variable.

3.2.1 *k-ε* model

Launder and Spalding in 1974 proposed *k-ε* turbulence model [3]. The *k-ε* turbulence model uses two model equations one for *k* and one for *ε*. The *k* and *ε* define the velocity scale (v) and length scale (l) representative of the large scale turbulence. The model assumes that the turbulent viscosity (μ_t) is linked to the turbulent kinetic energy (*k*) and dissipation (*ε*) via the relation given in Eq. 3.14.

$$\mu_t = C\rho v l = C_\mu \rho \frac{k^2}{\varepsilon}; \quad v = k^{1/2}, \quad l = \frac{k^{3/2}}{\varepsilon} \qquad (3.14)$$

*C*μ is a dimensionless constant whose value is 0.09. The *k* and *ε* values can be obtain from transport equations of turbulent kinetic energy (Eq. 3.15) and dissipation rate (Eq. 3.16).

$$\frac{\partial(\rho k)}{\partial t} + \frac{\partial}{\partial x_j}(\rho U_j k) = \frac{\partial}{\partial x_j}\left[\left(\mu + \frac{\mu_t}{\sigma_k}\right)\frac{\partial k}{\partial x_j}\right] + P_k - \rho\varepsilon + P_{kb} \qquad (3.15)$$

$$\frac{\partial(\rho \varepsilon)}{\partial t} + \frac{\partial}{\partial x_j}(\rho U_j \varepsilon) = \frac{\partial}{\partial x_j}\left[\left(\mu + \frac{\mu_t}{\sigma_\varepsilon}\right)\frac{\partial \varepsilon}{\partial x_j}\right] + \frac{\varepsilon}{k}\left(C_{\varepsilon 1}P_k - C_{\varepsilon 2}\rho\varepsilon + C_{\varepsilon 1}P_{\varepsilon b}\right) \qquad (3.16)$$

P_k denotes the turbulence production due to viscous forces and is given as in Eq. 3.17.

$$P_k = \mu_t \left(\frac{\partial U_i}{\partial x_j} + \frac{\partial U_j}{\partial x_i} \right) \frac{\partial U_i}{\partial x_j} - \frac{2}{3} \frac{\partial U_k}{\partial x_k} 3 \left(\mu_t \frac{\partial U_k}{\partial x_k} + \rho k \right) \qquad (3.17)$$

P_{kb} and $P_{\varepsilon b}$ represent the influence of the buoyancy forces. If the full buoyancy model is used, the buoyancy production term P_{kb} is given as in Eq. 3.18 and if Boussinesq buoyancy model is being used the production term P_{kb} is given as in Eq. 3.19. $P_{\varepsilon b}$ is assumed to be proportional to P_{kb} and must be positive is given in Eq. 3.20.

$$P_{kb} = \frac{\mu_t}{\rho \sigma_\rho} g_i \frac{\partial \rho}{\partial x_i} \qquad (3.18)$$

$$P_{kb} = \frac{\mu_t}{\rho \sigma_\rho} \rho \beta g_i \frac{\partial T}{\partial x_i} \qquad (3.19)$$

$$P_{\varepsilon b} = \max\left(0, P_{kb}\right) \qquad (3.20)$$

3.2.2 RNG k-ε model

The Standard *k-ε* is, widely established and used. It shows moderate agreement in non-limiting flows, curved boundary layers and eddy flows [2]. Reason of Bradshaw et al. in 1981 that the effects of the spread of pressure is not neglected [5].RNG (Renormalization group) supports *k-ε* in the normalization of group analysis for Navier-Stokes equations proposed by Yakut et al. In 1992 [6]. They represent effects of small turbulence due to random impact. RNG process systematically removes small scales movement of the prevailing equations by changing the impact in terms of larger Scales movements and changed viscosity. Typical equations and basic transports are the same as standard model *k-ε*, but the model constants differ, and the

$C\mu$constants in Eq. 3.14 is replaced by $C_{\mu RNG}$ and $C_{\varepsilon 1}$in Eq.3.16 has been replaced by the function $C_{\varepsilon 1RNG}$. The transport equation for turbulence dissipation is given in Eq. 3.21 [6].

$$\frac{\partial(\rho\varepsilon)}{\partial t}+\frac{\partial}{\partial x_j}\left(\rho U_j\varepsilon\right)= \frac{\partial}{\partial x_j}\left[\left(\mu+\frac{\mu_t}{\sigma_{\varepsilon RNG}}\right)\frac{\partial\varepsilon}{\partial x_j}\right]+\frac{\varepsilon}{k}\left(C_{\varepsilon 1RNG}P_k-C_{\varepsilon 2RNG}\rho\varepsilon+C_{\varepsilon 1RNG}P_{\varepsilon b}\right) \quad (3.21)$$

Where,

$$C_{\mu RNG}=0.0845\,,\qquad C_{\varepsilon 1RNG}=1.42-f_\eta\,,\qquad C_{\varepsilon 2RNG}=1.68$$

$$f_\eta=\frac{\eta\left(1-\frac{\eta}{4.38}\right)}{\left(1+\beta_{RNG}\eta^3\right)}\,,\quad \eta=\sqrt{\frac{P_k}{\rho C_{\mu RNG}\varepsilon}}\,,\qquad \beta_{RNG}=0.012$$

3.2.2 The shear stress transport (SST) turbulence model

In the *k*-*ε* model, the turbulent viscosity is expressed as a product of velocity and length scale as given in Eq. 3.14. The eddy viscosity in this case is given as in Eq. 3.22.

$$\mu_t=\frac{\rho k}{\omega};\quad \omega=\varepsilon/k \qquad (3.22)$$

Menter noted the results of *k*-*ε* turbulence model are much less sensitive to the assumed values in free stream but its near wall performance is unsatisfactory for boundary layers with the diverse pressure gradients [1],[9]. He suggested a hybrid model using [10], [11], [13].

(a) Transformation of *k*-*ε* turbulence model into a *k*-*ω* turbulence model in the near wall region.
(b) The standard *k*-*ε* turbulence model in the fully turbulent region far from the wall.

The digital instability can be caused by the difference in the calculated values of troubled viscosity with the standard k-standard far and near wall. Therefore, a blending function *F*1 is used as given in Eq. 3.23.

$$\phi = F_1\phi_1 + (1 - F_1)\phi_2 \qquad (3.23)$$

3.3 Energy Equation

The energy equation results from the first law of thermodynamics, which states that the average energy turnaround corresponds to the rate at which the heat is added to Liquid particles in addition to the work carried out on the liquid particle [1]. Surface forces determine the velocity of work on the liquid molecule and added heat to it. The whole energy equation is in Eq. 3.24.

$$\frac{\partial(\rho h_{tot})}{\partial t} - \frac{\partial p}{\partial t} + \nabla(\rho U h_{tot}) = \nabla\cdot(\lambda\nabla T) + \nabla\cdot(U\cdot\tau) + U\cdot S_M + S_E \qquad (3.24)$$

3.3.1 Thermal energy equation

The thermal energy equation is an alternative form of the energy equation and can be derived by subtracting the mechanical energy equation from total energy equation. The mechanical energy equation can be obtained by taking a dot product of *U* with momentum equation [4]. The thermal energy equation is given as in Eq. 3.25.

$$\frac{\partial(\rho h)}{\partial t}-\frac{\partial p}{\partial t}+\nabla\cdot(\rho U h)=\nabla\cdot(\lambda\nabla T)+U\cdot\nabla p+\tau:\nabla U+S_E \qquad (3.25)$$

3.3.2 Conjugate heat transfer

When conductive solids are contained in the liquid solution area flow and heat, usually referred to as the associated heat transfer problem. In the fixed ranges, the calculation of the energy equation can calculate the thermal transfer by fixed motion, conductivity, and volumetric heat sources. The energy equation for the steel field is in Eq. Indicated 3.25.

$$\frac{\partial(\rho h)}{\partial t}+\nabla\cdot(\rho U_s h)=\nabla\cdot(\lambda\nabla T)+S_E \qquad (3.25)$$

3.4 Summary

The details of the physical models used for pressurizer surge line thermal stratification has been described in detail, ANSYS CFX has been employed for CFD simulations. The brief details of governing equations for conservation of mass, momentum, turbulence models, energy and thermal energy equations are discussed.

The governing equations employed by ANSYS CFX are discussed in detail. The two equation turbulence models mainly standard k-ε, RNG k-ε and SST are discussed with advantages and limitations. Both RNG k-ε and SST turbulence models can provide improved results than standard k-ε turbulence model but later has an edge with less computation time versus requirements

Chapter 4

Analysis Verification and Validation

4.1 Introduction

The pressurizer surge line in reality is not only a straight pipe; it consists of vertical sections and bends in addition to horizontal section. Therefore it is deemed necessary to analyze the complete pressurizer surge line model for thermal stratification condition. Any CFD simulation needs to verified and validated. The verification of CFD results can be done through comparison with the experimental results or through validated codes or through known good published data. The last verification option is selected for this study, since the experimental results are not available. Further the published data also provide with the geometric dimensions and layout of pressurizer surge line which is scarce in available literature. The validation of CFD results is a complex process, which starts from CFD tool. ANSYS CFX, a commercially available known validated tool is used for CFD analysis. The next step is the correct setup of problem. The problem was setup keeping in view the necessary constraints. The turbulent behavior of flow is analyzed with SST instead of standard k-ε since the pressurizer surge line has curvilinear sections and standard k-ε turbulence model is known to be insensitive to streamline curvatures. The pressurizer surge line grid is discretized keeping in view the importance of near wall known and these regions are finely meshed. The overall grid is finer in radial and circumferential direction, whereas, to some extent coarse along the length of pressurizer surge line. The full buoyancy model is selected to cater for density difference.

4.2 Verification Procedure

The verification is carried out through comparison of study results with known good results. Jo et al. [1] simulation results are used for verification. Once the

simulation is verified the same scheme can be used for modified models of pressurizer surge line. To enhance the accuracy of verification process all possible known facts are incorporated. For instance a similar pressurizer surge line model, as depicted in Fig 27, geometric configuration, layout and material properties are used. Further, the same boundary conditions and flow conditions are used in simulation. The grid is discretized in accordance with the standard layout of ANSYS ICEM and same time step size is used. The same overall convergence criterion is used.

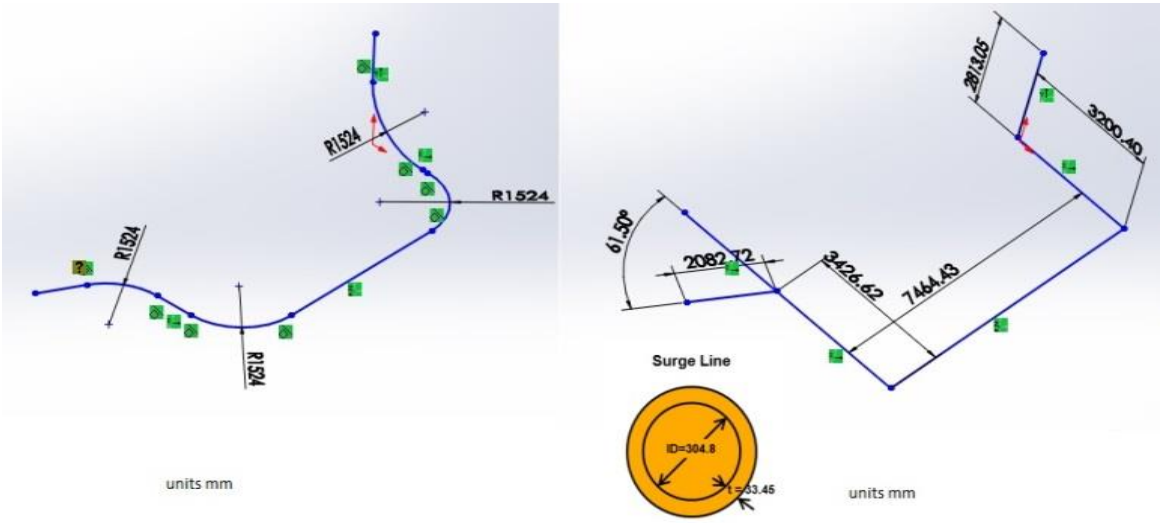

Figure 27 Pressurizer surge line geometric configuration and layout

4.3 Pressurizer surge line configuration, layout and properties

The pressurizer surge line model by Jo et al. [1] is used for the verification of simulation. The geometric configuration and layout is depicted in Fig 27 and Fig 28 respectively.

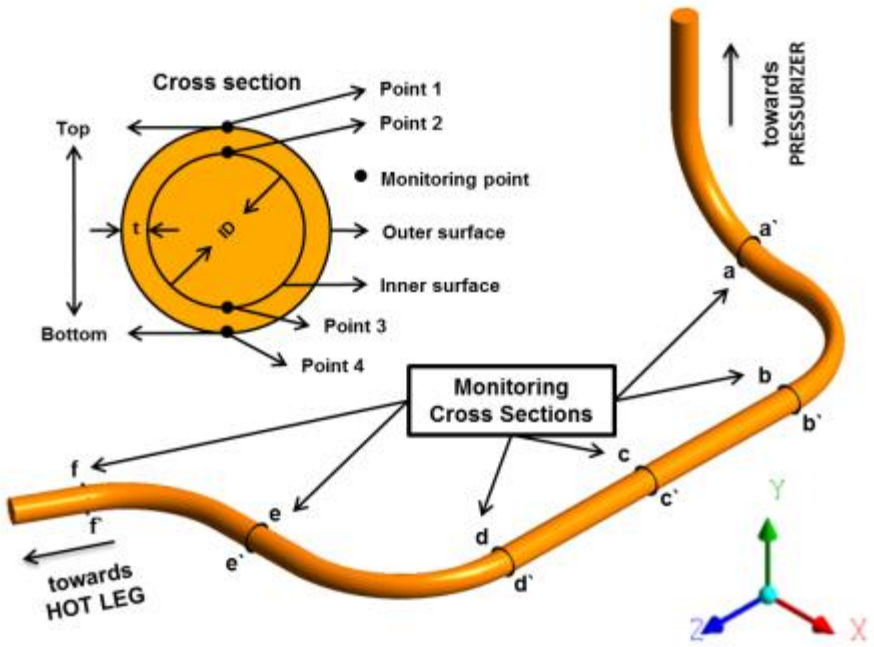

Figure 28 Pressurizer surge line monitoring points and cross sections

The pipe material is same as used by Jong Chull Jo et al. [1]. The monitoring point and cross sections are depicted in Fig 28. The monitoring points are at same locations i.e. top and bottom of pipe wall surfaces. However, the monitoring cross sections are approximately selected to be as close as possible by Jo et al. [1].

4.4 Problem Statement

The solution domain consists of pipe, which is divided into fluid and solid domains. The pipe wall thickness is considered as solid domain and flow field inside the pipe is taken as fluid domain. The CFD analysis is performed using conjugate heat transfer in order to consider the fluid structure interaction. Conduction heat transfer occurs in solid domain while both conduction and convection heat transfer in fluid domain. The outer wall surface of solid domain is considered as adiabatic i.e. no heat in or out from the pipe. The out surge case is consider and the cold fluid present in

pressurizer surge line is at 51.7 ^{0}C with reference pressure of 2.2408 MPa. After some time hot water from pressurizer at 218 ^{0}C starts flowing inside pipe with velocity of 0.07 m/s. The mixing of hot and cold water results in stratified flow and the fluid layers arranges itself due to density difference.

4.5 Problem Setup

In the current flow problem Reynolds number lies between ($0.38x10^{5}$< Re < $1.2x10^{5}$), which shows that flow is turbulent. Full buoyancy model is used for evaluation of density difference [5]. Scalable wall function is used to treat the flow near wall. The y+ value is in between 4 to 122 while, the solver y+ value is in between 12.08 to 27.

4.6 Grid Discretization

The fluid and solid domain of the model is discretized into 282,724 hexahedral elements. Regions near the fluid solid interface boundary are finely meshed as shown in Fig 29. To obtain realistic results hexahedral type elements are used. The overall mesh quality is maintained within the specified range based on ANSYS ICEM mesh quality criteria [3] [4].

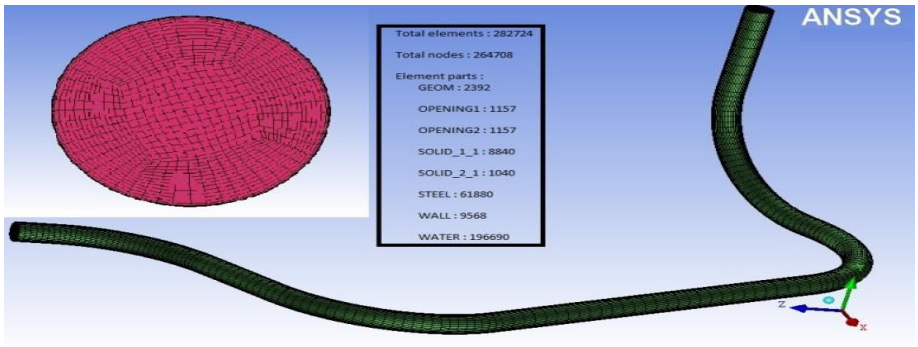

Figure 29 Pressurizer surge line meshing in ICEM

4.7 Sensitivity Test

The sensitivity test is performed to get optimum values for number of elements. The known optimum values of number of elements are than used to study stratified flow in pressurizer surge line.

4.7.1 Grid independency test

To make the results independent of mesh four different numbers of elements are used. The number of elements is in between282,724and 594,840with time step size of 1s.The temperature monitored at cross-section a-a` with different number of elements are shown in Table 5 .The temperatures values do not change much but high computation time is required even if the number of elements is increased above 282,724. Hence the optimum number of elements for out-surge case is selected as 282,724.

Table 5Temperature with respect to element numbers

Monitoring point	Temperature k-ε	Temperature RNG k-ε	Temperature SST	Cross Section	Number of elements	Simulation time
TOS	429.85K	425.74K	446.95K	a-a`	282,724	200 s
BOS	379.80K	359.52K	332.56K	a-a`	282,724	200 s
TOS-BOS	50.05	66.20	114.39	a-a`	282,724	200 s
TIS	481.90K	480.96K	482.13K	a-a`	282,724	200 s
BIS	464.62K	447.91K	370.22K	a-a`	282,724	200 s
TIS-BIS	17.28	33.05	111.91	a-a`	282,724	200 s
-	-	-	-	-	-	-
TOS	430.25K	423.31K	447.83K	a-a`	371,921	200 s
BOS	380.11K	360.02K	333.41K	a-a`	371,921	200 s
TOS-BOS	50.14	63.29	114.42	a-a`	371,921	200 s
TIS	482.95K	481.28K	482.94K	a-a`	371,921	200 s
BIS	465.14K	448.42K	370.51K	a-a`	371,921	200 s
TIS-BIS	17.81	32.86	112.43	a-a`	371,921	200 s
-	-	-	-	-	-	-
TOS	431.84K	424.44K	448.94K	a-a`	594,840	200 s
BOS	381.16K	360.18K	334.31K	a-a`	594,840	200 s
TOS-BOS	50.68	64.26	114.63	a-a`	594,840	200 s
TIS	483.92K	482.35K	483.84K	a-a`	594,840	200 s

BIS	466.08K	449.46K	371.21K	a-a`	594,840	200 s
TIS-BIS	17.84	32.89	112.63	a-a`	594,840	200 s

4.8 Comparison of Analysis Setup

The analysis setup of this study is described in the preceding text. An effort has been made during the analysis setup to harness as much as similarities possible. The comparison of the problem setup and simulation constraints with published data [1] is summarized in Table 6.

Table 6 Comparison of simulation constraints

S.NO	**Description**	**This study**	**Jo et al** [34]	**Remarks**
1	Pressurizer surge line layout	Figure 27	Figure 21	Identical
2	Pressurizer surge line inner diameter	304.8 mm	304.8 mm	Identical
3	Pressurizer surge line wall thickness	33.45 mm	33.45 mm	Identical
4	Water properties	IPAWS	IPAWS	Identical
5	Fluid velocity	0.07 m/sec	0.07 m/sec	Identical
6	Cold water temperature	51.7 °C	51.7 °C	Identical
7	Hot water temperature	218.3 °C	218.3 °C	Identical
8	Reference pressure	2.2408MPa	2.2408MPa	Identical
9	Turbulence Model	SST	SST	Identical
10	Pressurizer surge line outer wall surface	Adiabatic	Adiabatic	Identical
11	Pressurizer surge line grid	282,724	230,000	Comparable

		elements	nodes	
12	Mesh element type	Hexahedral	Hexahedral	Identical
13	Convergence Criteria	RMS < 10^{-3}	RMS < 10^{-3}	Identical

4.9 Result and Discussion

The transient developments of the temperature difference between the top and bottom inner wall surfaces along the cross sections a-a`, b-b`, c-c`, d-d`, e-e` and f-f` are depicted in Fig 30.Initially, there is no temperature difference since the hot fluid just starts flowing in the surge line and is far away from the monitoring cross sections due to low flow velocity of 0.07 m/sec. A steep change in temperature difference can be seen with its onset since the hot fluid has reached the monitoring cross section and due to density difference occupies the upper region of pressurizer surge line whereas the lower region of the pressurizer surge line is still occupied with the cold fluid. The top to bottom temperature difference reaches it maximum and then starts to reduce gradually owing to ample fluid mixing. The maximum temperature difference of 146 °C is observed across the cross section a-a`, which is near to the pressurizer end. Further it is also seen that the farther the monitoring cross section from the pressurizer end the lower the top to bottom temperature difference. This is merely due the heat transfer between the fluid molecules through convection and thus elevating the bulk fluid temperature. The transient developments of the temperature difference between the top and bottom inner wall surfaces along the cross sections a-a`, b-b`, c-c`, d-d`, e-e` and f-f` with and without wall of published data [1] are depicted in 31.The maximum temperature difference between top to bottom inner wall surfaces is again observed at the cross section a-a` near to the pressurizer end. Moreover, the top to bottom temperature difference of inner wall surface remains above 125°C even after simulation time of 500s. In contrast the simulation results which predict reduction in top to bottom inner wall surface temperature as depicted below in Fig 30 along the monitoring cross section a-a’. The overall length of pressurizer surge line is 12.2 m with a flow velocity of

0.07 m/s, the surging fluid can complete more than two length cycles during the considered simulation time of 500s. Hence, the fluid mixing is imminent.

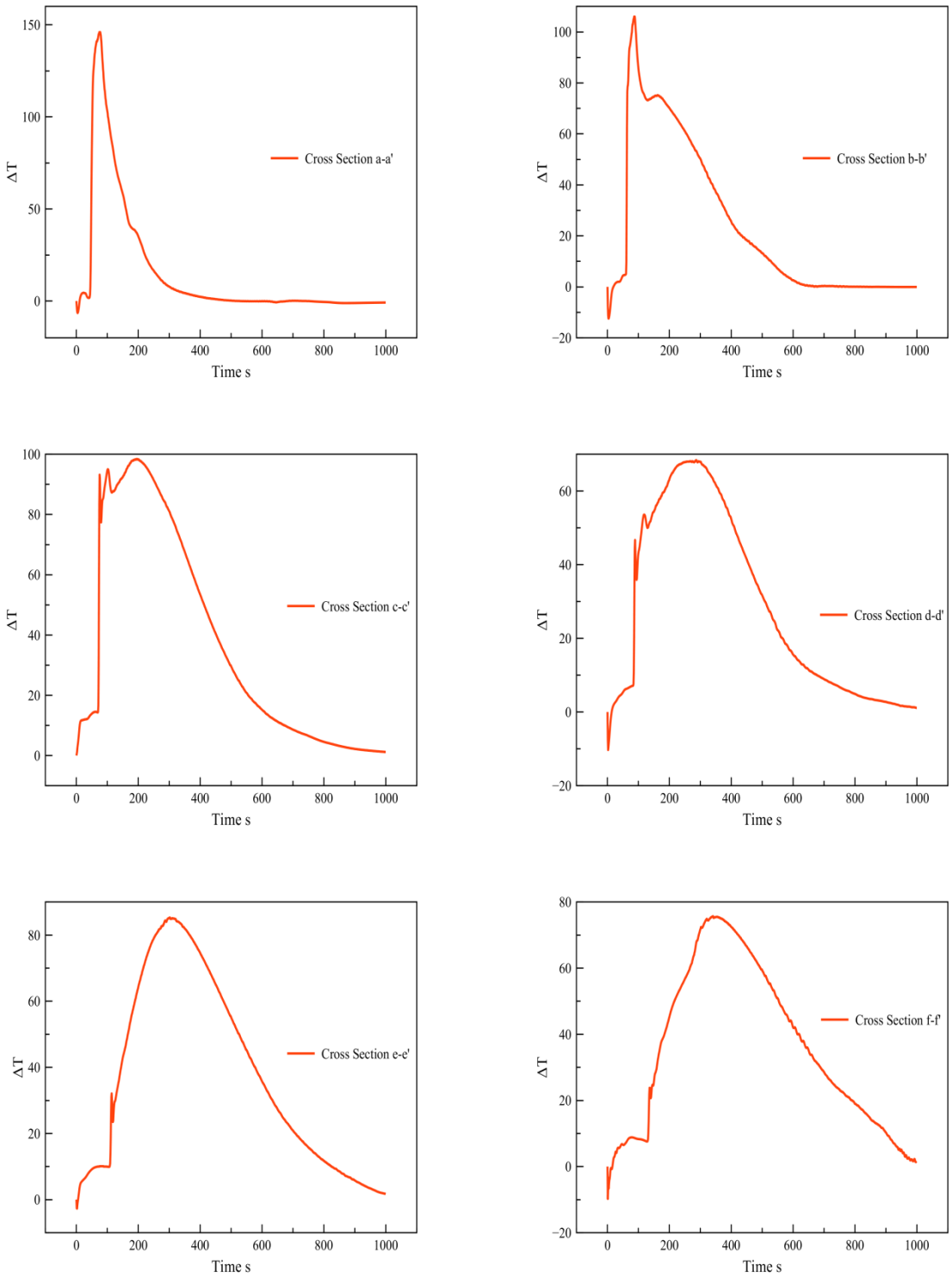

Figure 30 Transient progression of temperature differences between top and bottom inner wall surfaces of the cross section a-a` through f-f`.

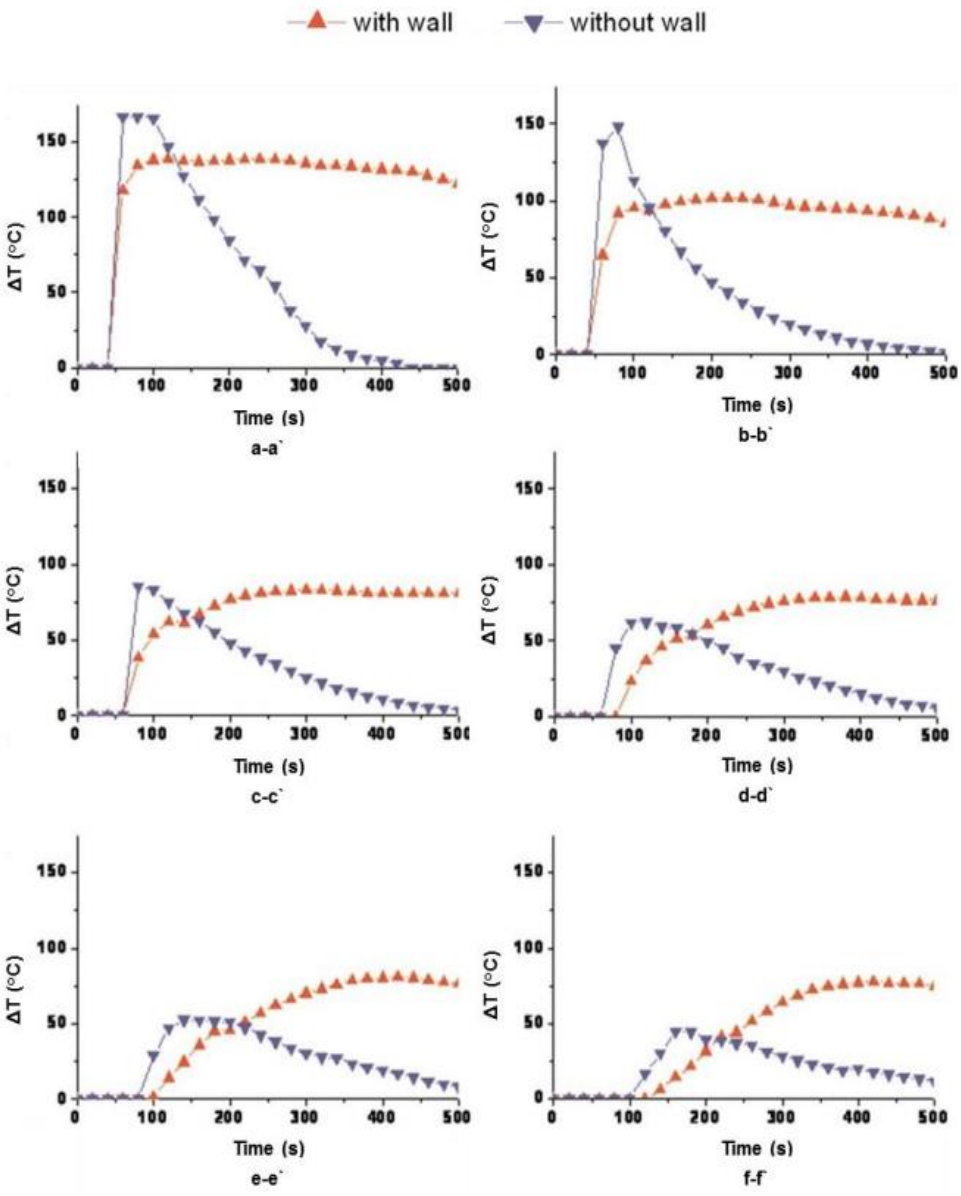

Figure 31
Transient progression of temperature differences between top and bottom inner wall surfaces of the cross section a-a` through f-f` [1].

The simulation results are also compared with published data of Kim et al [2] depicted in figure 32. They simulated the heat up phase for the pressurizer surge line of Ulchin Unit 5 and 6. The pressurizer surge line has an inner diameter of 329 mm and thickness of 33.3 mm nearly similar to this study analysis model dimensions, whereas the geometric layout is different. They have observed an increase in top to bottom temperature difference with an increase of flow rate with They have observed the maximum top to bottom temperature difference of

115°C along the monitoring cross-section location (9A) near to the pressurizer end, for flow rate of 30 gallons per minute (0.022 m/s) as depicted in Fig 32, which is comparable to the results of this work depicted above in Fig 30.

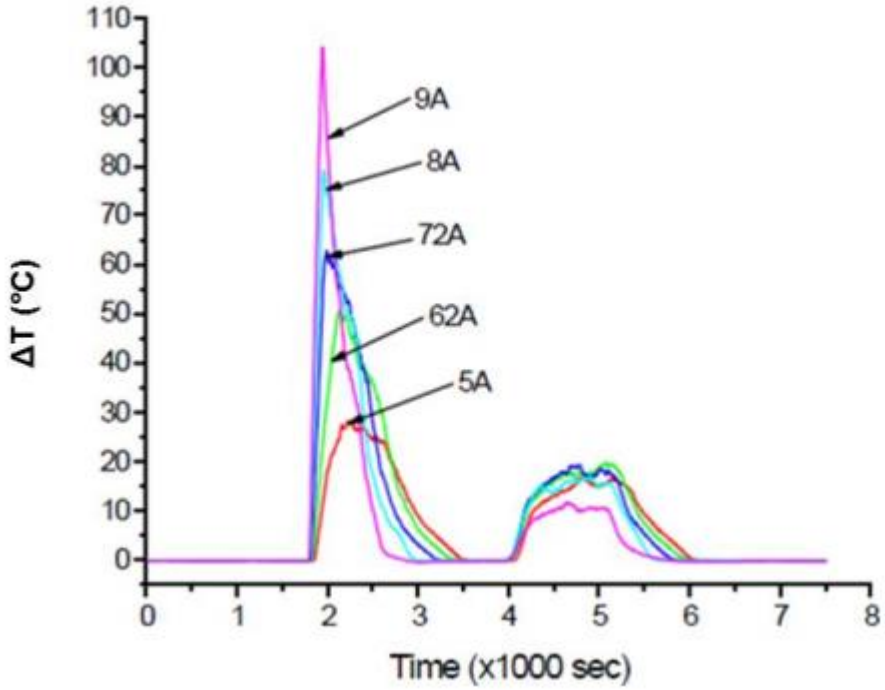

Figure 30Top to bottom temperature difference for heat up rate of 30 gpm [2]

4.10 Summary

The validation and verification of CFD simulation is carried out in this chapter. ANSYS CFX, a commercially available known validated tool is used for CFD analysis. The simulation constraints and corresponding results are compared. The maximum temperature difference from top to bottom inner wall surface of about 146 °C is observed across the monitoring cross section a-a` near to the pressurizer end which is comparable with the published results of temperature difference around 145°C [1] and 110°C [2].An anomaly is observed while comparing the transient temperature profile of inner wall surface temperature difference. The transient top to bottom inner wall surface results initially predict a steep increase

in temperature difference with onset simulation time of 40 s until it reaches the maximum value of around 146°C and then the temperature difference reduces smoothly with elapsed time to a value of about 20°C at the simulation time of 500 s.The published data [1] predicts a similar onset of steep increase in temperature difference at about simulation time of 40 s with maximum of 145°C.However, the published data [1] displays almost constant temperature profile maintaining a temperature difference of above 125°C. The deviation in results in light of heat transfer fundamentals is discussed. The simulation results of the transient top to bottom inner wall surface temperature difference profile along the monitoring cross section a-a` near to the pressurizer end are compared with the published data [2] and are found to be in acceptable agreement.

Chapter 5

CFD Analysis of Pressurizer Surge Line

5.1 Introduction

The thermal stratification phenomenon in pressurizer surge line is common due to the temperature difference between the fluid entering from pressurizer end and fluid entering from hot leg end. This difference in temperature causes density difference and hence warmer lighter fluid flows over cooler heavier fluid resulting in flow stratification. The pressurizer surge line has complex geometry. It runs down vertically and horizontally with varying slopes and curvatures connecting pressurizer with the hot leg of the primary coolant loop. [1].Therefore, to develop an understanding of thermal stratification a realistic model is used. Moreover the effect of flow velocity or heat up rate on thermal stratification is also studied. Three different heating up rates are achieved by varying the inlet flow velocity. Furthermore, the choice of turbulence model among selected two equations turbulence models is also discussed. The pressurizer surge line is also analyzed for over all downward slope of 5 degree.

5.2 Operating Condition of PWR

The PWR operates at high pressure and temperature. Shah and Conley [7] discussed that during heat up the temperature difference of the fluid can be as high as 180°C. The hot leg coolant temperature is normally 54°C before starting the coolant pumps. While, the pressurizer coolant temperature can be as high as 218°C corresponds to lower pressure of 2.24 MPa. Grebner and Hofler discussed that during heat up the temperature difference of the fluid can be as high as 150°C. Shah and Conley [7] also discussed that tendency of stratified flow is greatest during heat up and cool down phases of reactor operation because of the large temperature difference. However, the occurrence of thermal stratification in pressurizer surge line has been mostly reported for heat up phase [3], [4], [5]. The complete heat up phase is a lengthy process. It generally takes about 8-10

hours from reactor shut down condition. It can be simulated in stages for simplicity and computational effort. The initial stage is considered till the fluid temperature reaches 218°C. Generally, the fluid temperature in shut down condition is maintained in range of 50 to 55°C. The pressure remains constant during the considered initial phase till fluid temperature of 218°C is achieved and a continuous out surge from pressurizer end is maintained.

5.3 Problem Statement and Setup

The present problem is the same as mentioned in chapter 4. The similar procedure for problem setup is used as discussed in chapter 4. Three cases with different flow velocities are considered. The governing equations are given in chapter 3.The geometrical data and properties of pipe material and fluid are given in Table 7.

Table 7 Paremetric Values

Parameter	Value
Material of the pipe	ASME SA-312
Inner diameter (ID) of the pipe	305 mm
Thickness (t) of the pipe	33.5 mm
Density of the pipe	8000 Kg/m^3
Thermal conductivity of the pipe	16.3 W/m-K
Specific heat capacity of the pipe	500 J/kg-K
Thermal expansivity of the pipe	$17e^{-6}$ /K
Fluid (water)	IAPWS IF97
Initial Temperature of the fluid	51.7 ^oC
Inlet Temperature of fluid	218 ^oC

Reynolds number for the flow	$0.283x10^5$ - $1.05x10^5$

5.4 Boundary conditions

Typical out surge case is considered for pressurizer surge line. The initial bulk temperature of fluid is set to 51.7°C.The inlet fluid temperature is consider to be 218°C with a flow velocity of 0.05 m/s . The reference pressure is maintained to 2.2408MPa.The outer surface of the pipe is considered as adiabatic. The solid domain is initialize with 25°C and fluid domain is initialize with inlet flow velocity for each case. The monitor cross sections and monitor points used for analysis are shown in Figure 33.

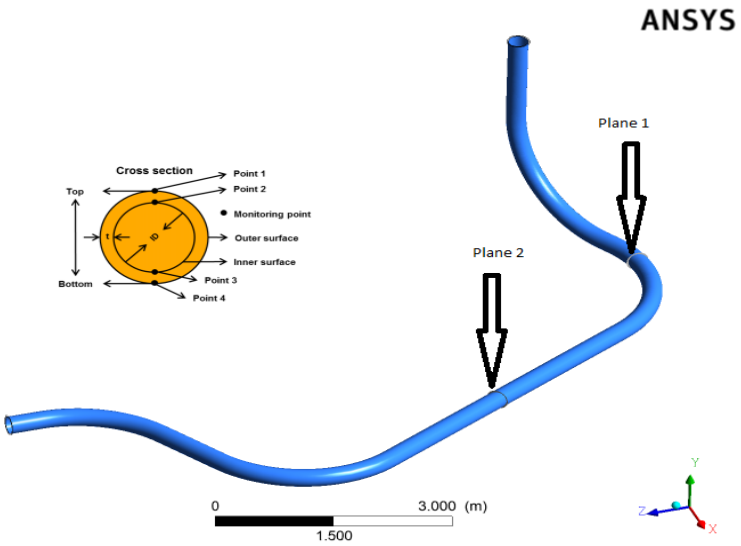

Figure 31 Pressurizer surge line monitoring points and cross sections

5.5 Result and Discussion

The time dependent temperature variation for inner and outer surfaces are presented and discussed in light of turbulence models, fluid velocity, over all downward slope and thermal stratification.

5.5.1 Choice of Turbulence Model

The turbulence behavior of fluid flow in pipe is simulated using standard SST, RNG k-ε and k-ε models. The temperature differences for inner wall surfaces of the three turbulence models at flow velocity of 0.05 m/s are shown in Figure 34.The cold fluid (51.7 °C) present in pressurizer surge line and hot fluid (218 °C) starts flowing inside pipe thus resulting a high temperature difference in the start of simulation. The hot fluids with lesser density accumulate in the top of pipe thus increasing the top surface

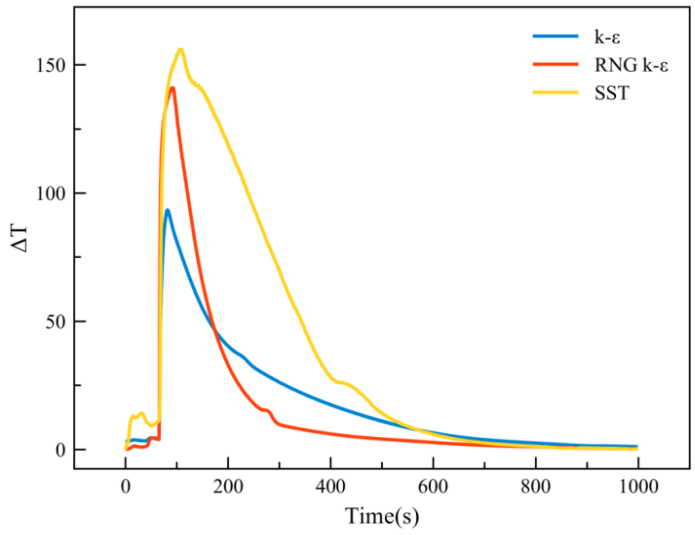

Figure 32 and bottom inner wall surface temperature difference at flow velocity of 0.05 m/s

temperature and resulting a large inner wall surfaces temperature differences. The out surging hot fluid in pressurizer surge line keep increasing the bulk fluid temperature which results in increase of bottom inner wall surface temperature. The increase of fluid bulk temperature reduces the inner wall surfaces temperature differences. Thus with the passage of time the stratification effect reduce considerably and temperature difference is minimum after simulation time of 600s.The temperature difference curves of top and bottom inner wall surfaces start rising at simulation time of 65s.The highest top and bottom inner wall surface temperature difference is observed for SST (156 °C) as compared to k-ε (93 °C) and RNG k-ε (140 °C) turbulence models. The outer wall surface

temperature difference for the three turbulence models at flow velocity of 0.05 m/s is shown in Figure 32.

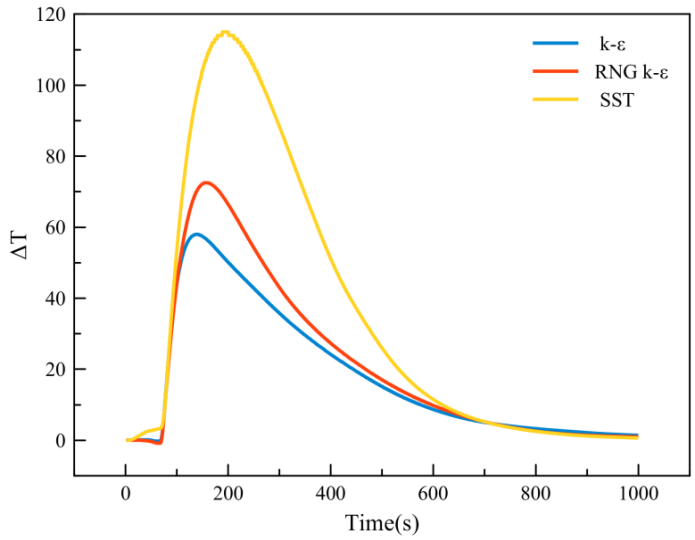

Figure 33 Top and bottom outer wall surface temperature difference at flow velocity of 0.05 m/s

The temperature difference curves for top and bottom outer wall surfaces rise initially at simulation time of 70 s and gradually decrease with passage of time for the three turbulence models. The temperature difference curves for outer wall surfaces develop slowly as compare to inner wall surfaces because of heat transfer. The out-surging fluid in pressurizer surge line transfer heat via convection, while conduction takes place between inner and outer wall surfaces. The convection heat transfer is much quicker than conduction heat transfer. The highest top and bottom outer wall surface temperature difference is observed for SST (115 °C) as compared to k-ε (58 °C) and RNG k-ε (72 °C) turbulence models. The bulk fluid temperature in pressurizer surge line slowly homogenizes which results in large outer wall surfaces temperature differences. The transient temperature distribution of top inner wall surface (TIS), bottom inner wall surface (BIS), top outer wall surface (TOS) and bottom outer wall surface (BOS) for different turbulence models are shown in Figure 34,35,36 ,37 , 38 and 39 .

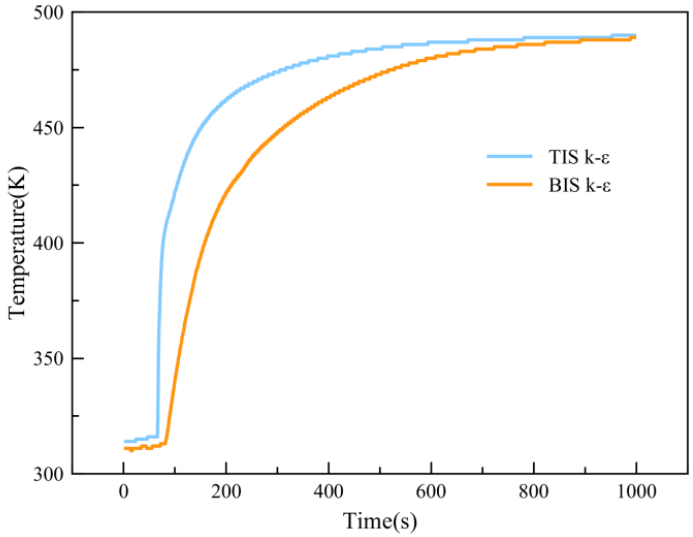

Figure 34 TIS and BIS for k-ε model at flow velocity of 0.05 m/s plane 1

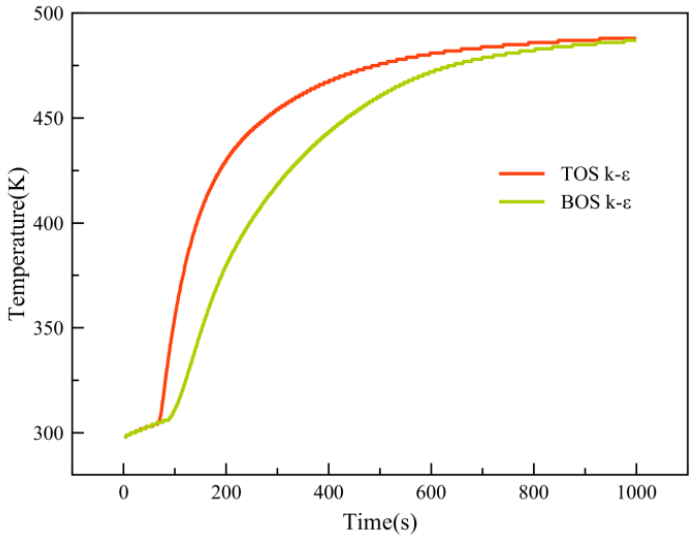

Figure 35 TOS and BOS for k-ε model at flow velocity of 0.05 m/s plane 1

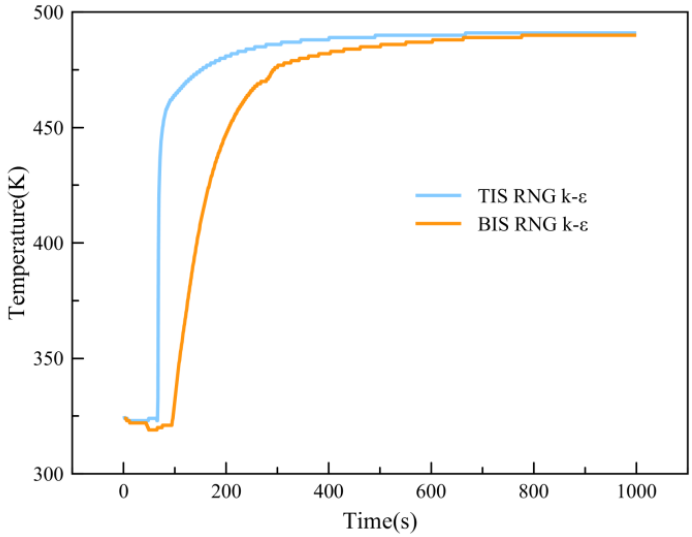

Figure 36 TIS and BIS for RNG k-ε model at flow velocity of 0.05 m/s plane 1

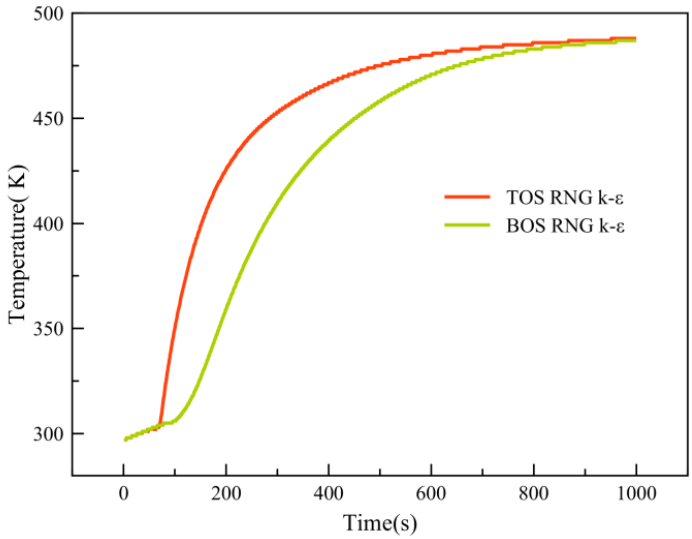

Figure 37 TOS and BOS for RNG k-ε model at flow velocity of 0.05 m/s plane 1

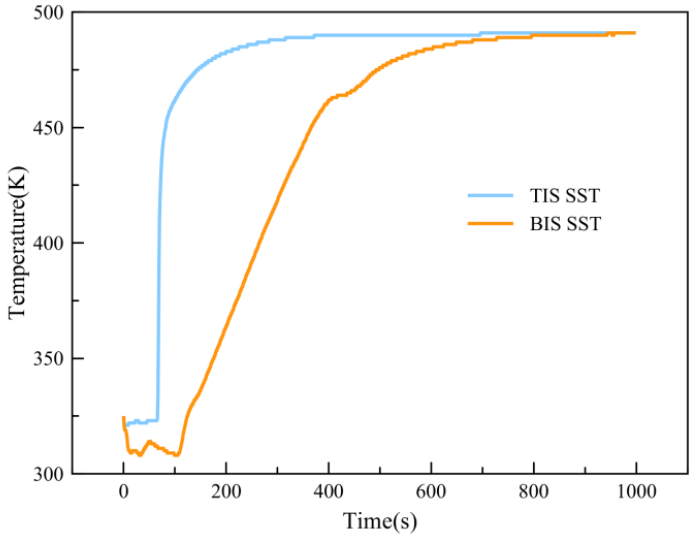

Figure 38 TIS and BIS for SST model at flow velocity of 0.05 m/s plane 1

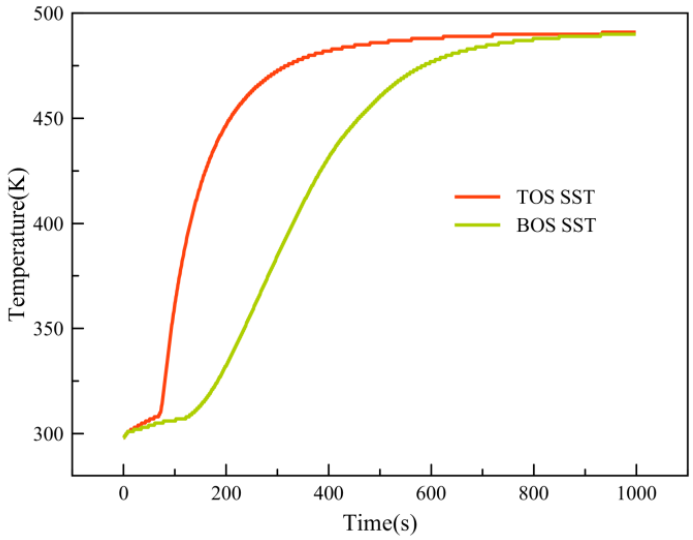

Figure 39 TOS and BOS for SST model at flow velocity of 0.05 m/s plane 1

The transient temperature distribution depends on the turbulence model used. The inner and outer wall surfaces temperature differences are highest for SST turbulence model. The standard k-ε and RNG k-ε shows comparable inner and outer wall surfaces temperature differences after simulation time of 200s.The temperature differences for inner and outer surfaces at 200s are shown in Table 8.It is clear from the Table 8 that SST turbulence model predicts highest temperature difference for both inner and outer wall surfaces as compare to RNG

k-ε and k-ε for simulation time of 200s.The pressurizer surge line is not a straight pipe it has curvilinear sections. The standard k-ε turbulence model is insensitive to streamline curvatures. Both SST and RNG k-ε turbulence models known to have accuracy with swirling flows. Therefore, RNG k-ε and SST turbulence models are best choice to capture the accurate turbulent fluid flow behavior in pressurizer surge line under thermal stratification condition. The computational time for similar simulation conditions are significantly less for RNG k-ε turbulence model.

Table 8 Three models inner and outer surfaces temperature differences at 200s for plane 1

	Temperature		
	standard k-ε	**RNG k-ε**	**SST**
TOS	429.85K	425.74K	446.95K
BOS	379.80K	359.52K	332.56K
TOS-BOS	50.05	66.20	114.39
TIS	481.90K	480.96K	482.13K
BIS	464.62K	447.91K	370.22K
TIS-BIS	17.28	33.05	111.91

5.5.2 Effect of flow velocity

The pressurizer surge line is evaluated with flow velocity of 0.05 m/s, 0.1 m/s and 0.2 m/s. The turbulent fluid flow behavior is evaluated with SST turbulence model. The inner wall surfaces temperature differences for the mention flow velocities are shown in Figure 37.It is observed that at lower flow velocity of 0.05 m/s the conduction heat transfer between fluid molecules is more significant than convection heat transfer. The conduction heat transfer is slower as compare to convection therefore, the temperature difference is sustain for longer period of

time which results in stable stratification effect in pressurizer surge line. The fluid temperature homogenize slowly for lower fluid velocity due to conduction heat transfer between fluid molecules. Hence, inner wall surfaces temperature differences drop slowly for fluid velocity of 0.05 m/s. The convection heat transfer is dominant for higher flow velocity because of fluid mixing therefore, fluid temperature is homogenized quickly due to quicker mode of heat transfer

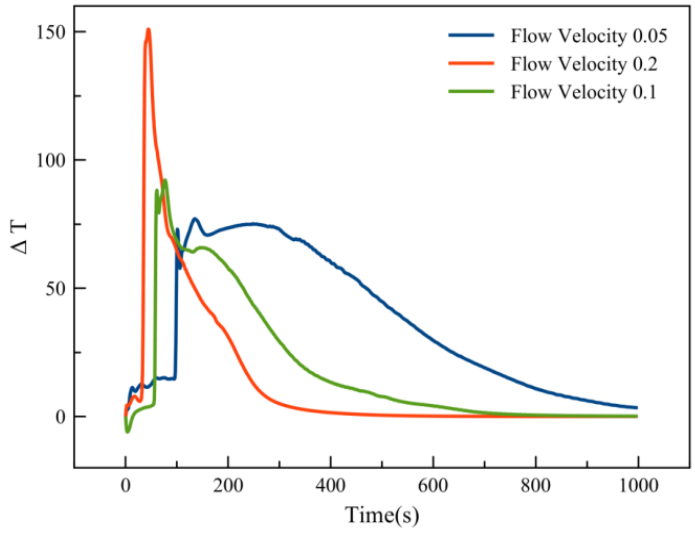

Figure 40 Inner wall surfaces temperature differences for 3 flow velocities at plane 2

Hence, inner wall surfaces temperature differences drops quickly for higher flow velocity of 0.1 m/s and 0.2 m/s. The inner wall surfaces temperature differences (Figure 40) time span is shown in Table 9.The pressurize surge line have curvilinear sections which facilitates turbulence in fluid flow. This turbulence is not enough to dismiss stratification effect in pressurizer surge line; however with higher flow velocity the turbulence can increase the heat transfers rate up to some extent. The reason for highest peak of temperature difference curve in Figure 40 is due to turbulence effect at high flow velocity. In Table 9 the temperature difference is higher for flow velocity of 0.2 m/s as compare to flow velocities of 0.05 m/s and 0.1 m/s.

Table 9 Time span of temperature difference curves for inner wall surfaces at plane 2

Fluid velocity	ΔT rise time	ΔT end time	Time span	Maximum ΔT
0.05 m/s	95s	903s	808s	77.13 ^0C
0.1 m/s	53s	674s	621s	92.21 ^0C
0.2 m/s	29s	332s	303s	151.34 ^0C

The outer wall surfaces temperature differences for the mention flow velocities are shown in Figure 41.

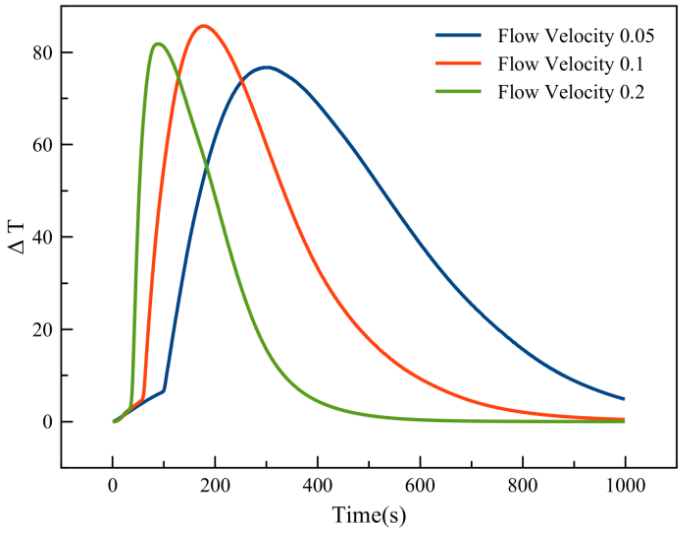

Figure 41 Outer wall surfaces temperature differences for 3 flow velocities at plane 2

The outer wall surfaces temperature differences curves are much smoother. The temperature difference curves initially increases with increase in flow velocity and later decrease with increase in flow velocity. The slower mode of conduction heat transfer exist between the wall surfaces which results in smoother progression of temperature difference. Similarly the initial increase in outer wall surfaces temperature differences is due to conduction heat transfer between the

wall surfaces. The transient temperature distribution of TIS, BIS, TOS and BOS for different flow velocities are shown in Figure 42,43,44,45 and 46.

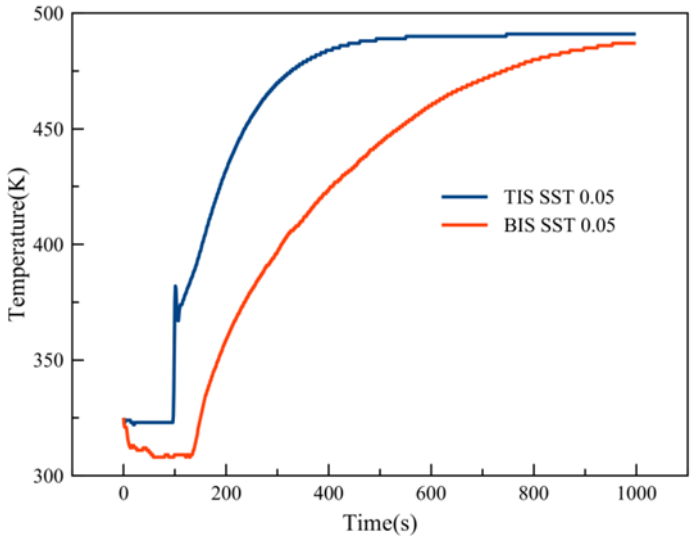

Figure 42 TIS and BIS for SST model at flow velocity of 0.05 m/s plane 2

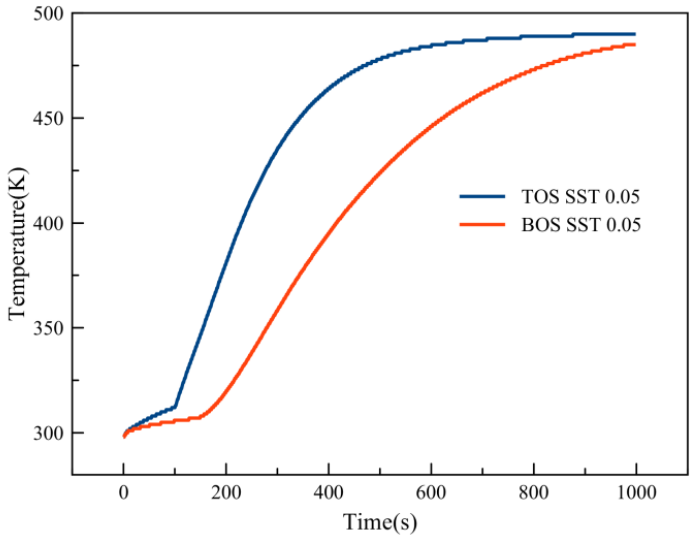

Figure 43TOS and BOS for SST model at flow velocity of 0.05 m/s plane 2

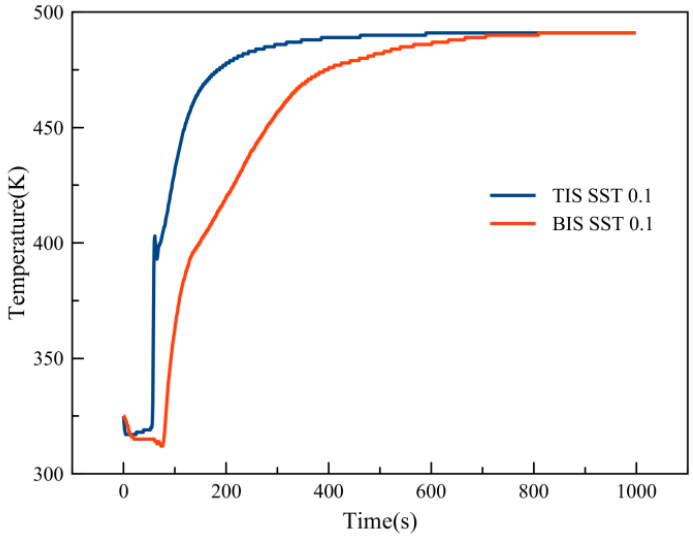

Figure 44 TIS and BIS for SST model at flow velocity of 0.1 m/s plane 2

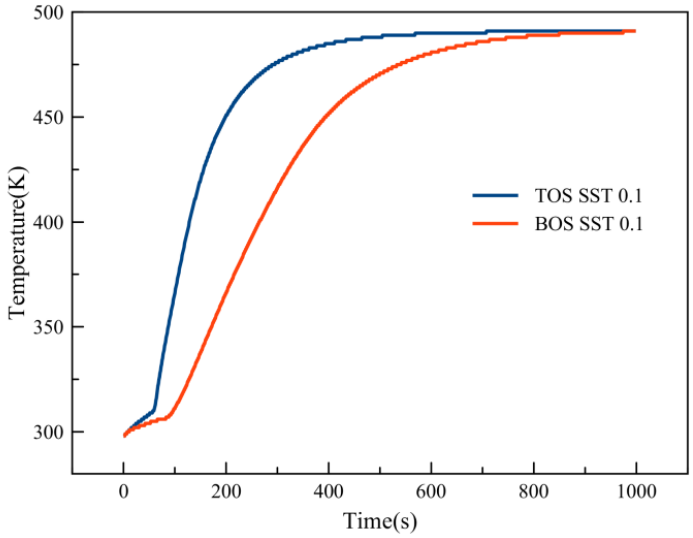

Figure 45 TOS and BOS for SST model at flow velocity of 0.1 m/s plane 2

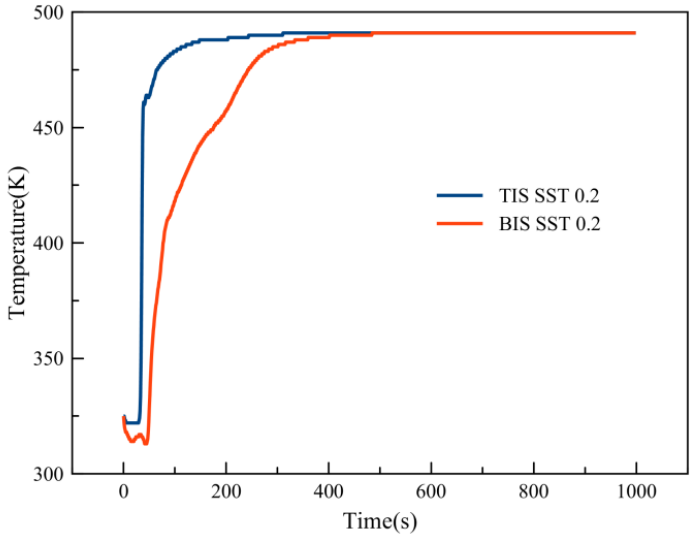

Figure 46 TIS and BIS for SST model at flow velocity of 0.2 m/s plane 2

The temperature difference is maximum for top inner wall surface because the hot fluid occupy in the upper region of pipe. The inner and outer wall surfaces temperature homogenize swiftly with increase in flow velocity.

Time s	Flow velocity 0.05 m/s	Flow velocity 0.1 m/s	Flow velocity 0.2 m/s
120	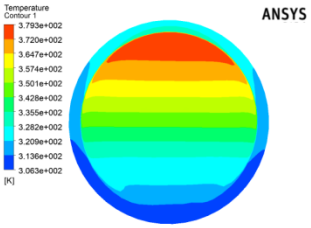	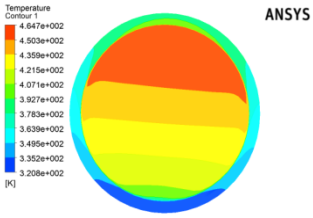	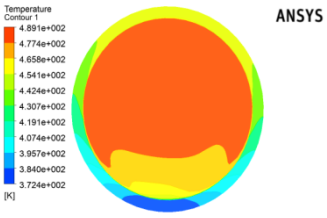
220	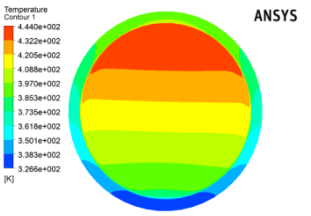	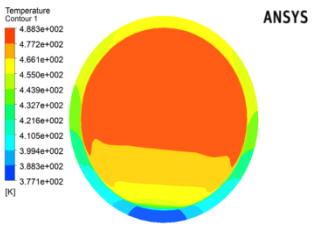	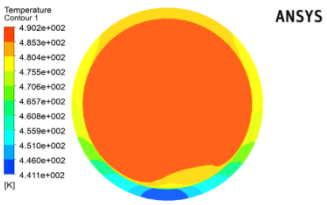
420	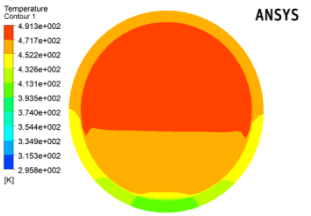	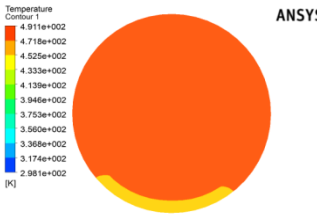	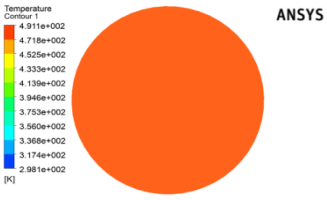
1000	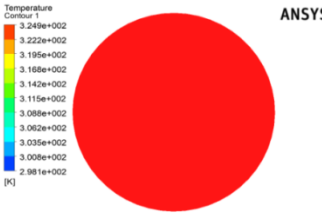	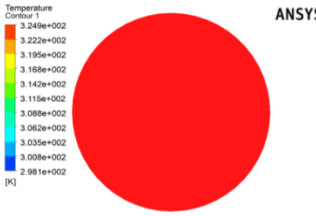	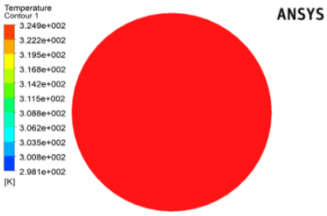

The transient temperature distribution for different heat up rates at simulation time of 120s, 220s, 420s and 1000s are shown in Figure 40. The temperature distribution is uniform at higher flow velocities because the out surging fluid sweeps the entire length of pressurizer surge line. It is observed that at lower flow velocity for which the Richardson number is very high, the flow is highly stratified. The Richardson numbers are given in Table 10. The stratification effect reduces at high heat up rate due to low Richardson number. The results obtained verify the dependency of stratification phenomenon on Richardson number.

5.5.3 Over all Downward Slope of 5 Degree

The pressurizer surge line layout may help in mitigation of thermal stratification phenomenon and therefore, the effect of overall downward slope is considered in preceding text. The pressurizer surge line model with hot leg is modified to attain an overall downward slope of five degree starting from the horizontal section and of pressurizer surge line as depicted in Fig 47.

The problem statement, setup and grid discretization is same as described above. The transient evolution of top to bottom inner wall surface temperature differences for pressurizer surge line model with an overall downward slope of five degree is depicted in Figure 48.

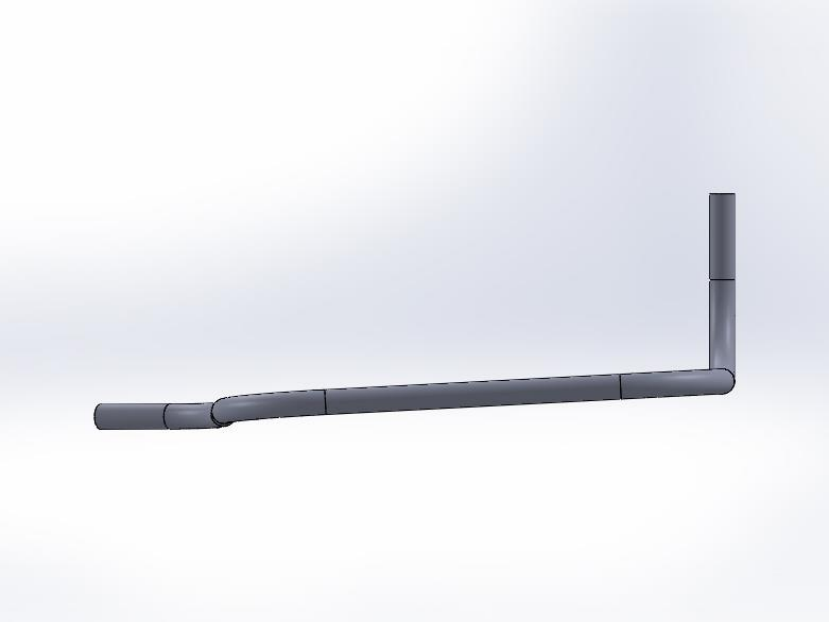

Figure 47 Pressurizer surge line model with downward slope of five degree

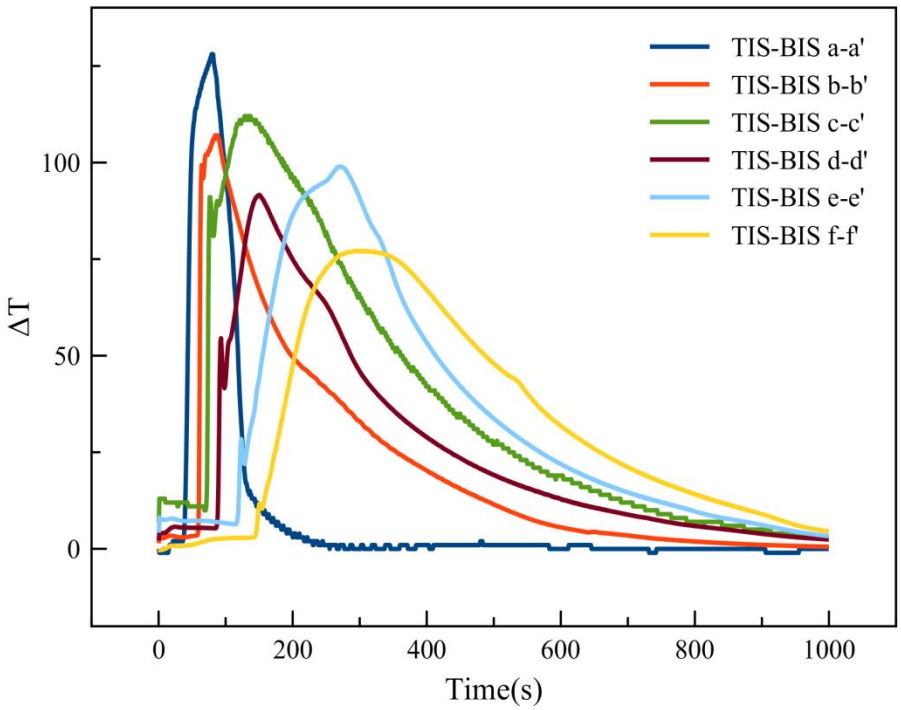

Figure 48 top to bottom inner wall surface of pressurizer surge line model with an overall slope of 5 degree

The maximum top to bottom temperature difference is observed along the monitoring cross section a-a` which is near to the pressurizer end. The overall temperature difference reduces with an increase in distance the pressurizer end with maximum of about 107 °C and around 98°C along the monitoring cross sections b-b` and c-c` respectively. There after the trend of temperature difference increases with maximum of about 91°C and around 86°C along the monitoring cross sections d-d` and e-e` respectively and then again reduces along the monitoring cross section f-f` with the maximum of about 77°C. This abrupt change in trend of top to bottom inner wall surface temperature difference is mainly due to the introduction of downward slope in the pressurizer surge line model. To further evaluate this varying trend of top to bottom temperature difference along the monitoring cross sections near the out let top and bottom inner wall surface temperatures are shown in figure 49 and 50 respectively.

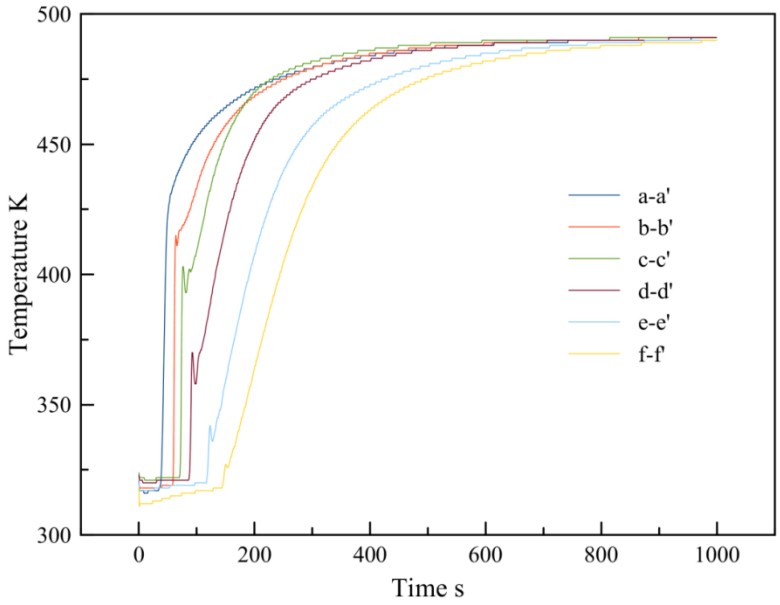

Figure 49 TIS for different cross sections with over all downward slope of 5 degree

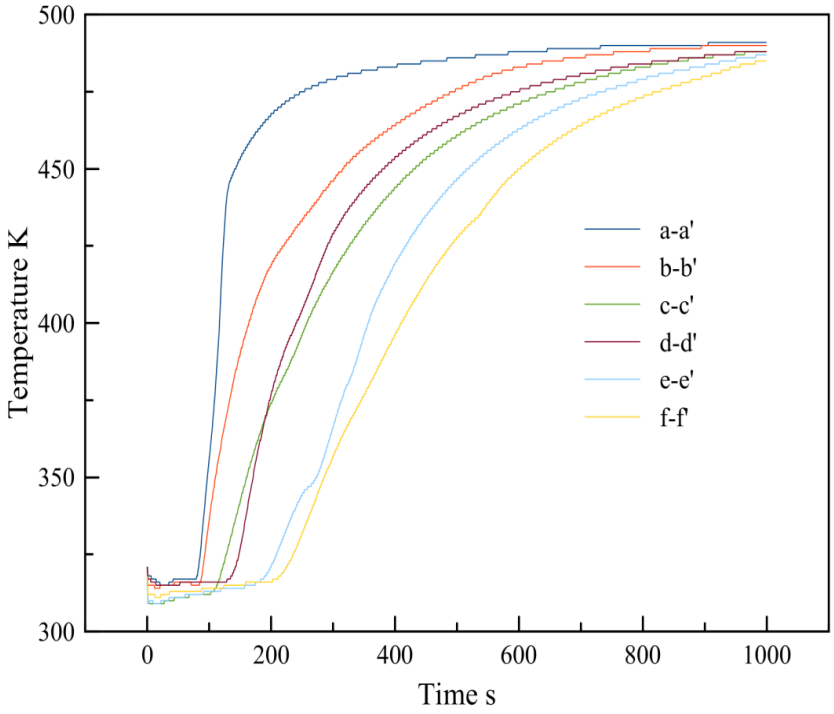

Figure 50 BIS for different cross sections with over all downward slope of 5 degree

The top inner wall surface temperature of monitoring cross sections c-c` (210°C),d-d` (208°C) and e-e` (201°C) increases uniformly to near inlet fluid temperature of218°C whereas at monitoring cross section f-f` a lower temperature of 146°C is observed mainly due to mixing effect. The bottom inner wall surface temperatures of monitoring cross sections c-c`(190°C) and d-d`

(180°C) increases uniformly towards the inlet fluid temperature of218 °C whereas at monitoring cross section e-e` and f-f` a lower temperature of134°C and 99°C is observed due to fluid mixing.

5.6 Summary

In this chapter study is conducted to understand the thermal stratification in PWR surge line. The three mentioned two equation models have different temperature differences for inner and outer wall surfaces at same simulation conditions. The temperature difference is highest for SST as compared to RNG k-ε and standard k-ε turbulence models. The standard k-ε turbulence model shows lowest temperature difference and its limitation to stream line curvatures make it least favorable option. The RNG k-ε and standard k-ε models shows comparable results after simulation time of 200s.The RNG k-ε and SST models can be used to study thermally stratified flow in pressurizer surge line however, simulation time is significantly less for RNG k-ε as compare to SST. The SST model is combination of k-ε and k-ω turbulence models and correctly predicts the amount of flow separation from smooth surfaces [1] therefore, SST model is the best suited for current problem with the trade-off in simulation time. The flow velocity significantly affects the stratification in pressurizer surge line. The stratification effect of fluid flowing in pressurizer surge line depends on Richardson number. The fluid with lower flow velocity and high Richardson number shows stable stratification effects as compared to higher flow velocity with lower Richardson number. The time span of temperature difference for thermal stratification effect is minimum at higher flow velocity as compare to lower flow velocity. Generally thermal stratification effect is reduced as flow velocity is increased which shows the dependence of thermal stratification on Richardson number.

The pressurizer surge line model is modified to achieve and overall slope of 5 degree. It is observed that it reduces the top to bottom temperature difference between the inner wall surface near the pressurizer end and with an increase in distance from pressurizer end this temperature difference increases. The overall downward slope does not greatly influence the flow and temperature field in regions nearest to out let of pipe.

The thermal stratification is one of the main issues for PWR pressurizer surge line. The future designs of pressurizer surge should be improve to minimize the thermal stratification effects by considering the turbulence effect of fluid flowing inside the pipe. The turbulence of fluid flow depends on geometric layout and out surging flow velocity of pressurizer surge line. A very high flow velocity will facilitate instantaneous thermal shocks because of very high temperature difference and can damage the structural integrity of pipe. The pressurizer surge line should be design for optimum diameter and length to attain optimum flow velocity.

Conclusions

The study is conducted to develop and understanding of the thermal stratification phenomena of pressurizer surge line for pressurized water reactor. The study is performed through numerical. The simulation procedure is validated; simulation results are verified against published data and found to be in an acceptable agreement.

The effects of flow velocity on thermal stratification in a straight pipe are discussed. The turbulent behavior of flow is analyzed with three different turbulence models namely, standard k-ε, RNG- k-ε, and SST turbulence models. Modification in overall slope of pressurizer surge line is incorporated in analysis. The results are presented and discussed. The study on pressurizer surge line thermal stratification is concluded with following key points.

1. A stratified flow is observed in the pressurizer surge line of pressurized water reactor.
2. The heat up rate affects the thermal stratification phenomenon, at very low flow velocities of the order of 0.05 m/sec the top to bottom temperature difference increases and later with increase in flow velocity this difference decreases. Overall, the increase in heat up rate reduces the tendency of thermal stratification phenomenon.
3. The RNG K-E and SST turbulence models can be used to analyze the behavior of flow in pressurizer surge line for thermal stratification condition. The well established and most widely validated standard k-ε turbulence

model does not predict well due to its moderate agreement in unconfined flows, curved boundary layers and swirling flows.

4. The overall downward slope in the pressurizer surge line affects the flow field and reduces the maximum top to bottom temperature difference along the
   pressurizer surge line especially in regions near pressurizer end.

Apropos, to above it is recommended that the new designs of pressurizer surge line may address the overall downward slope in the pressurizer surge line to mitigate the effects of thermal stratification. Further, an increase in heat up rate may also help in mitigation of thermal stratification phenomenon.

References

Chapter 1

Introduction

[1] Wikipedia. Industrial Revolution. 2012,
URL: http://en.wikipedia.org/wiki/Industrial_Revolution

[2] American Nuclear Society Nuclear news. Fifty years ago in December: Atomic Reactor EBR-I produced first electricity. November 2001,
URL: http://www.ans.org/pubs/magzines/nn/docs/2001-11-2.pdf

[3] US Department of Energy, Argonne National Laboratory. Reactors designed by Argonne National Laboratory: Fast Reactor Technology. 2012,
URL: http://www.ne.anl.gov/About/reactors/frt.shtml

[4] International Atomic Energy Agency. From Obninsk beyond: Nuclear Power Conference Looks to Future. June 2004,
URL: http://www.iaea.org/newscenter /news/2004/obninsk.html.

[5] IAEA. Nuclear Power Reactors in the World 2012 Edition: Reference Data Series 2. June 2012, Vienna, Austria: International Atomic Energy Agency. .

[6] "https://www.nei.org/Knowledge-Center/Nuclear-Statistics/World-Statistics."

[7] "https://www.euronuclear.org/info/encyclopedia/n/npp-reactor-types.htm."

[8] Wikipedia. Pressurized Water Reactor. 2012,
URL: http://en.wikipedia.org/wiki/Pressurized_water_reactor

[9] US Energy Information Administration. Nuclear & Uranium: Pressurized Water Reactor and Reactor Vessel. 2012,

URL: http://www.eia.gov.cneaf/nuclear/page/nuc_reactors/pwr.html

[10] H. Grebner and A. Holler. Investigation of Stratification effects on the Surge Line of a Pressurized Water Reactor, ELSEVIER Computers & Structures, 1995, 56: 425-437.

[11] C. Ensel , A. Colas , M. Barthez. Stress Analysis of a 900 MW Pressurizer Surge Line including Stratification Effects. Nuclear Engineering and Design. 1995, 153: 197-203.

[12] Nitin J. Shah, Keshab K. Dwivedy. Risk-Based Inspection of Pressurizer Surge Lines. Proceedings of SPIE – The International Society for Optical Engineering. 1996, 2947: 59-66

[13] Yu, Y.J., Sohn, Y.S., Park, S.H. and Bak, W.J. Evaluation of surge line thermal stratification and implementation to piping design. Transactions of SMiRT 13, Brazil. 1995, 127-135.

[14] Y.J. Yu, J.H. Jheon, K.S. Yoon, and S.H. Park, Development of Piping Analysis Procedure of a PWR Surge Line for Stratified Flow, Journal of the Korean Nuclear Society. 1996, 28: 390-397.

[15] KINS. Development of Assessment Technology for Fluid-Structure Interaction using ANSYS (based on Surge Line due to Thermal Stratification), Korea Institute of Nuclear Safety. 2009, KINS/RR-700.

[16] IAEA. Assessment and Management of Ageing of Major Nuclear Power Plants Components Important to Safety, Primary Piping in PWRs. IAEATECDOC-1361. July 2003, Vienna, Austria: International Atomic Energy Agency.

Chapter 2

Literature Review

References

[1] USNRC Cracking in Feed Water System Piping. U.S. Nuclear Regulatory Commission Bulletin No. 79-13, Washington, DC. 1979..

[2] USNRC. Thermal Stresses in Piping Connected to Reactor Coolant Systems. U.S. Nuclear Regulatory Commission Bulletin No. 88-08, Washington, DC. 1988.

[3] USNRC. Unexpected Piping Movement Attributed to Thermal Stratification. U.S. Nuclear Regulatory Commission Information Notice No. 88-80, Washington, DC. 1988.

[4] J. USNRC. Pressurizer Surge Line Thermal Stratification. U.S. Nuclear Regulatory Commission Bulletin No. 88-11, Washington, DC. 1988.

[5] Ph. Taupin, E. Thomas-Solgadi, C. Ensel. Method to Assess Mechanical Effects of Stratification in Piping System. 10th International Conference on Structural Mechanics in Reactor Technology, SMiRT 10, Anaheim, CA, USA. 1989, 195-201.

[6] I. NKS. Stratification issues in the Primary System: Review of available validation experiments and State of the Art in modeling capabilities. Nordic Nuclear Safety Research NKS report 202, Roskilde, Denmark 2009.

[7] E. B. Liang. Periodic Remaining Life Evaluation Program of PWR Pressurizer Surge Line accounting for Thermal Stratification Effect. Proceedings of Second International Symposium on Nuclear Power Plant Life Management, Shanghai, 15-18 October 2007.

[8] USNRC. Standard Review Plan 3.9.3: ASME Code Class 1, 2, and 3 Components Supports, and Core Support Structures, Revision 2. 2007.

[9] P. Hirschberg and G. A. Ataki. Measurement of stratification in the pressurizer surge line: Design and Analysis of Piping Components – 1989. ASME Pressure vessel and piping conference, Honalulu, HI, USA, July 23-27, 1989, PVP169: 85-90.

[10] Timothy J. Griesbach, Peter C. Riccardella and Stephan R. Gosselin. Application of fatigue monitoring to the evaluation of pressurizer surge lines. Nuclear Engineering and Design. 1991, 129: 163-176.

[11] P.Yu, Y.J., Lee, T.H., Sohn, Y.S., Park, S.H. and Bak, W.J. Thermal stratification of surge line in PWR nuclear power plant. Proceedings of ASME PVP Conference. 1995, 304: 67-72

[12] P. Klaus W. Bieniussa, Hans Reck. Pipping specific analysis of stresses due to thermal stratification. Nuclear Engineering and Design. 1999, 190: 239-249

[13] J. F. M. White. Fluid Mechanics. 4th Edition. McGraw Hill.

[14] D. Y. A. Cengel. Heat Transfer A Practical Approach. 2nd Edition. McGraw Hill.

[15] Ill Seok Jeong and Man Heung Park. Thermal stratification in horizontal circular cylinder with external heat tracing. Numerical Heat Transfer, Part A. 1999, 35: 85-98.

[16] D. Jong Chull Jo, Yun II Kim and Seok Ki Choi. Numerical Analysis of Thermal Stratification in Circular Pipe. Journal of Pressure Vessel Technology. 2001, 123: 517-524.

[17] Ildiko Boros and Attila Aszodi. Analysis of thermal stratification in the primary circuit of VVER-440 reactor with CFX. Nuclear Engineering and Design. 2008, 238: 453-459.

[18] Young Jong Kim, Maan Won Kim, Hyun Soon Lee and Eunmi Ko. Effect of vertical pipe length on the thermal stratification in nuclear power plant surge line. Proceedings of ASME 2008 Pressure vessels and piping division conference. PVP2008-61501.

[19] Dong Gu Kang and Jong Chull Jo. CFD Analysis of thermally stratified flow and heat transfer in a pressurizer surge line. Proceedings of ASME 2008 Pressure vessels and piping division conference. PVP2008-61204.

[20] Jong Chull Jo and Dong Gu Kang. CFD analysis of thermally stratified flow and conjugate heat transfer in a pressurizer surge line. Journal of Pressure Vessel Technology. 2010, 132: 021301-1-10

[21] KINS. Development of assessment technology for fluid structure interaction using ANSYS (based on surge line due to thermal stratification). 2009, KINS/RR-700

[22] Young Jong Kim, Maan Won Kim, Eunmi Ko, Jae Gon Lee and Byoung Chul Kim. Effcet of heat-up transient condition on the thermal stratification in nuclear power plant surge line. Proceedings of ASME 2009 Pressure vessels and piping division conference. PVP2009-7804.

[23] Faisal Asfand. CFD simulation of thermal stratification in pressurizer surge line. Proceedings of Tenth International Congress of Fluid Dynamics. 2010, ICFD10-EG-3089.

[24] Zhangfei Qu and Xuewu Cao. Numerical analysis of thermal stratification in pressurizer surge line. Proceeding of the 18th International Conference on Nuclear Engineering. 2010, ICONE18-29278.

Chapter 3

Numerical Modeling

References

[1] H K Versteed and W Malalasekera. An introduction to computational fluid dynamics. The finite volume method. 2nd Edition, Pearson Education Limited, Essex, England, 2007

[2] H. Schilichting and K. Gersten. Boundary layer theory. 7th Edition, McGrawHill, Newyork, USA, 1979.

[3] B. E. Launder and D.B. Spalding. The numerical computation of turbulent flows. Computer methods in applied mechanics and engineering. 1974, 3-2: 269-289

[4] ANSYS. ANSYS CFX-Solver theory guide. ANSYS Inc. 2010

[5] P. Bradshaw, T. Cebeci and J. H. Whitelaw. Engineering calculation methods for turbulent flow. Academic press London, 1981.

[6] V. Yakhot, S. A. Orszag, S. Thangam, T. B. Gatski and C. G. Speziale. Development of turbulence models for shear flows by a double expamsion technique. Physics of fluids A. American institute of physics. 1992, 4-7: 1510-1520

[7] D. C. Wilcox. Comparison of two equation models for boundary layers with pressure gradients. Journal of American institute of aeronautics and astronautics. 1993, 31-8: 1414-1421

[8] D. C. Wilcox. Simulating transition with two equation turbulence models. Journal of American institute of aeronautics and astronautics. 1994, 32: 247-

[9] F. R. Menter. Performance of popular turbulence models for attached and separated adverse pressure gradient flows. Journal of American institute of aeronautics and astronautics. 1992, 30: 2066-2072

[10] F. R. Menter. Improved two equation k-ω turbulence models for aerodynamics flows. NASA technical memorandum TM-103975, 1992.

[11] F. R. Menter. Two equation eddy viscosity turbulence model for engineering applications. Journal of American institute of aeronautics and astronautics. 1994, 32: 1598-1605

[12] F. R. Menter, M. Kuntz and R. Langtry. Ten years of industrial experience with the SST turbulence model. Proceedings of the fourth international symposium on turbulence, heat and mass transfer. Begell House, Redding, CT. 2003

[13] K. Mohanarangam, T. V. Nguyen and D. W. Stephens. Evaluation of two equation turbulence models ina laboratory scale thickner feed wall. Proceedings of seventh international conference on CFD in the minerals and processing industries, CSIRO, Melbourne, Australia. 2009.

Chapter 4

Analysis Verification and Validation

References

[1] Dong Gu Kang and Jong Chull Jo. CFD Analysis of thermally stratified flow and heat transfer in a pressurizer surge line. Proceedings of ASME 2008 Pressure vessels and piping division conference. PVP2008-61204.

[2] Young Jong Kim, Maan Won Kim, EunmiKo, Jae Gon Lee and Byoung Chul Kim. Effcet of heat-up transient condition on the thermal stratification in nuclear power plant surge line. Proceedings of ASME 2009 Pressure vessels and piping division conference. PVP2009-7804.

[3] ANSYS. ICEM CFD Manual. ANSYS Inc. 2010

[4] ANSYS. CFX Manual. ANSYS Inc. 2010

[5] ANSYS. ANSYS CFX-Solver theory guide. ANSYS Inc. 2010